

Adaptive Harvest-Then-Transmit for a Two-Tier Heterogeneous Wireless Network

by

Adedayo Ogundipe

A Thesis submitted to The Faculty of Graduate Studies of
The University of Manitoba
in partial fulfillment of the requirements for the degree of

Master of Science

Department of Electrical and Computer Engineering
University of Manitoba
Winnipeg

June 2016

Copyright © 2016 by Adedayo Ogundipe

Abstract

Multi-antenna techniques, energy harvesting, and the dense deployment of small cell base stations are some of the prominently discussed features of emerging and future wireless communication networks. Of particular interest is the subject of energy harvesting, where the possibility of powering end-user terminals of a cellular network from ambient sources, and specifically from Radio Frequency (RF) signals, has attracted significant attention from researchers who have published a sizeable amount of literature in the field in recent years. The benefits obtained from an energy self-sufficient communication network are numerous, both to operators and end users. End users derive a much enhanced user experience since the sustained availability of energy in the system ensures that network Quality of Service (QoS) parameters will always be met, device downtimes will be eliminated, user productivity will be increased and the inconveniences resulting from charging devices at fixed ports will be eliminated.

On the other hand, network operators will derive increased profits from services rendered as the number of users accessing their services on a continuous basis grow, while those with hierarchical cell deployments will benefit from energy savings as base station transmitters at different tiers do not transmit at levels that would have been the case for homogeneous networks even as cell-edge experience better service. To this end, this thesis examines minimum throughput maximization in a two-tiered wireless-powered communication network where a Hybrid Access Point (HAP) and Small Cell Base Station (SBS) coordinate downlink energy beamforming and uplink information processing with their associated users. I employed combined constraint optimization

to maximize both the minimum data rate of users at each tier and the minimum total rate for each user in the whole network, adopting two solution methodologies with an adapted Harvest Then Transmit (HTT) protocol at the SBS tier. My numerical results showed interesting results, including the fact that the optimal alternating optimization approach which utilizes MMSE beamformers outperforms the Zero-forcing alternative and that the optimal time parameter setting at the first tier does not necessarily ensure that the desired objective for the second and overall network can be met. They also show how spectral radius balancing is performed and how the solution methods employed perform power allocation so as to overcome the doubly near-far phenomena in wireless-powered communication networks (WPCNs).

Acknowledgements

I am immensely grateful to my supervisor, Professor Ekram Hossain, for the support, empathy and guidance that he provided me during the time of my studies at the University. I appreciate the camaraderie enjoyed by all of us on the WiCoNs research team and the opportunity to acquire knowledge alongside very bright colleagues of mine, particularly my pals Amr Abdelnasser, Amin Ghazanfari and also my good friend Zhen Zhao.

I thank my friend David Jegede for facilitating my admission into the University of Manitoba, my wife for keeping the home front particularly during engrossing study times, my parents for supporting me ever since my birth, and God almighty for directing the course of my life, to him be all the praise.

Table of Contents

List of Figures	iv
List of Tables	v
List of Abbreviations	vi
Publications	vii
1 Introduction	1
1.1 Wireless Power Transfer	2
1.1.1 Wireless Power Transfer Techniques	3
1.2 Energy Harvesting	5
1.2.1 Energy Harvesting: Sources	5
1.2.2 Energy Harvesting: Receiver Architecture	11
1.2.3 Energy Harvesting for SBSs	13
1.3 Multi-Antenna Techniques	13
1.4 Heterogeneous Networks	17
1.5 Motivation	18
1.6 Problem definition	19
1.7 Related Work	19
1.8 Contribution	21
1.9 Organization of Thesis	22
2 Mathematical Preliminaries	24
2.1 Mathematical Optimization	24
2.1.1 Convex optimization: Introduction	25
2.1.2 Convex optimization problem: Definition	27
2.2 CVX	28
2.2.1 Disciplined Convex Programming	29
2.3 Array Math	31
2.3.1 Definitions	31
2.3.2 Array Operations	32

3	Adapted Harvest-Then-Transmit for a two-tier HetNet: MMSE decoders	34
3.1	System Model and Assumptions	34
3.1.1	DL WET to HAPUs	36
3.1.2	DL WET to SBS and SCUs	37
3.1.3	UL WIT Phase	38
3.2	Problem Formulation	39
3.3	Solution Methodology	40
3.3.1	Background and Problem Simplification	40
3.3.2	Perron Frobenius Theorem	41
3.3.3	Equivalent Spectral Radius Minimization Formulation	42
3.4	Performance evaluation	48
3.4.1	Simulation parameters	48
3.4.2	Numerical results	49
3.5	Summary	53
4	Adapted HTT for HetNets: Zero-Forcing decoders	55
4.1	Background	55
4.2	Problem Formulation	57
4.3	Performance evaluation	60
4.4	Summary	62
5	Conclusion and Future Work	63
5.1	Conclusion	63
5.2	Future Work	64
	References	65

List of Figures

1.1	Energy Harvester Schematic [1]	11
1.2	Transmit Beamforming	16
1.3	Receive Beamforming	17
3.1	A two-tier HTT HetNet.	35
3.2	(a) R_k vs. τ_1 , (b) R_s vs. τ_2 for different τ_1 .	50
3.3	(a) 3D view of R_{Tot} vs. τ_1 for different τ_2 , (b) Different view of (a).	51
3.4	(a) R_k vs. Nr. of HAP Antennas (b) R_{Tot} vs. Nr. of HAP Antennas	52
3.5	(a) HAP tier SINR balancing, (b) SBS tier SINR balancing.	53
4.1	(a) Tier 1 power allocation, (b) Tier 2 power allocation, $\tau_1 = 0.1$.	60
4.2	(a) R_k vs τ_1 :MMSE vs ZF, (b) R_{Tot} vs τ_2 , $\tau_1 = 0.4s$.	61
4.3	R_k vs P_{Tot} : MMSE vs ZF	62

List of Tables

2	Scholastic works	vii
1.1	Wireless Power Control Techniques [1] [2]	4
1.2	Energy Harvesting Sources [1] [2] [3]	6
2.1	DCP Rules [30]	30

List of Abbreviations

CSI	Channel state information
DL	Downlink
HAP	Hybrid Access point
HTT	Harvest Then Transmit
HTT	Harvest Then Transmit
IP	Internet Protocol
MIMO	Multiple-Input Multiple-Output
QoS	Quality of Service
SBS	Small Cell Base Station
SINR	Signal-to-interference-plus-noise ratio
SISO	Single-Input Single-Output
TDMA	Time-Division Multiple Access
UL	Uplink
WET	Wireless Energy Transfer
WIT	Wireless Information Transfer
WPCN	Wireless-Powered Communication Network
w.r.t.	With respect to
LHS	Left hand side
RHS	Right hand side

Publications

S/N	Publication
1	Adedayo Ogundipe , Amr AbdelNasser, Ekram Hossain, “Cooperative Harvest-Then-Transmit in a Two-tier HetNet” submitted to the <i>IEEE Transactions on Vehicular Technology</i> .
2	Hina Tabassum, Ekram Hossain, Adedayo Ogundipe , “Wireless Powered Cellular networks Key Challenges and Solution Techniques”, <i>IEEE Communications Magazine</i> , vol.53, no.6, pp.63-71, June 2015

Table 2: Scholastic works

Chapter 1

Introduction

In order to meet the ever-changing throughput, delay, latency and other QoS requirements of modern communication networks, different ideas, techniques and technologies have been either proposed, tested or implemented. This is particularly justifiable given the anticipated spike in the amount of simultaneously connected devices expected to access services in such networks in the nearest future, with the Internet of Things (IoT) being an expected major contributor. Multi-antenna techniques, improved modulation schemes and waveforms, enhanced coding techniques, and the exploitation of new wide-band frequency spectra are some of these methods employed to meet these evolving demands, and one expects to see even more interesting approaches in the future.

However, one unintended consequence of fulfilling these QoS criteria is the increase in power consumption in these networks, particularly at end user terminals which are typically not powered by fixed sources. This is evidenced in the speed with which the batteries of these terminals, particularly those who usually access bandwidth-intensive services like gaming or video live streaming get drained out, a scenario which also plays out for users located at the fringes of these networks who typically

have to transmit at higher power so as to meet minimum service requirements. In a situation where billions of mobile devices are expected to operate at Gigabit speeds with the deployment of 5G and beyond-5G services, the relatively slow rate of battery technology evolution compared to the increase in energy consumption has made it imperative to find ways of guaranteeing energy self-sufficiency for these devices so as to ensure that they can operate not only at predefined QoS levels but also for lengthier periods than presently obtained. One area that has generated considerable interest recently as a plausible means to achieve this is energy harvesting from ambient sources. In the following sections, I discuss energy harvesting in details, showing how it can be used in conjunction with other techniques to increase the amounts of power available to users in a wireless communication network.

1.1 Wireless Power Transfer

In general terms, Wireless power transfer (WPT) is the process of conveying electrical energy without utilizing physical conductors from a transmitter which is typically connected to a fixed source of power through a conductive space to one or more receiving terminals, where the energy is harnessed by converting it into electrical form for use. In specific terms, WPT employs either time-varying electrical, magnetic or a combination of both fields to transmit energy from a transmitter to a receiver node. These ambient and time-varying fields, generated by alternating current (A.C) of electrons at the transmitting element (which could be a coil of wire, a metallic plate or even an antenna either of which produces a magnetic field, an electric field and electromagnetic waves respectively) propagates through a wireless medium to induce alternating current in the receiver element.

1.1.1 Wireless Power Transfer Techniques

Different methods are employed to facilitate wireless power transfer, differentiated mainly by the effective propagation distance of the transferred power and the oscillation frequency of the participating fields. In general, WPT techniques are classified into:

- **Non-radiative/Near field techniques:** These are used for power transfer within the immediate environment of the transmitter where the oscillating electric and magnetic fields are decoupled from each other. They are so-named because appreciable power can only be transmitted within the immediate region of the transmitter and if there is no receiver close-by, no effective WPT can take place. Examples of such techniques include magnetic or resonant coupling and capacitive coupling [1–4] which perform wireless power transfer via oscillating magnetic and electric fields respectively. Resonant coupling is used to transmit power between coils which are designed to vibrate at a particular frequency at both transmitter and receiver, since the possible energy transfer distance is increased if the coils at both ends vibrate at the same frequency. On the other hand, capacitive coupling involves the use of electric fields to transmit power usually between metal electrodes. The limitations of these techniques lie in the fact that the power transferred decays after at an exponential rate [4], specifically at about 60dB for every 10 meters, and also in the continuous need for recalibrating the coils at both transmitter and receiver ends.
- **Radiative/Far-field techniques:** are techniques employed in regions beyond 1 wavelength of the transmitter, where the high-frequency oscillating and magnetic fields generated by alternating current at source are perpendicularly

aligned (coupled) and as such circulate as electromagnetic (EM) waves, examples of which are light waves, microwaves, and radiowaves used in laser, satellite and radio communication respectively. The power transferred via far-field techniques decays with respect to the inverse of the distance between the transmitter and receiver elements, amounting to about 20dB for every 10 meters. Far-field techniques possess a number of advantages over near-field ones, these include the fact that they could be used to power several spatially dispersed users, they offer convenience and mobility to the end-users, and that the electromagnetic waves employed for power transfer could also be used to transmit information. Table 1.1 below provides more information about the near and far-field techniques discussed.

Technique	Field	Operating distance	Efficiency	Applications
Electromagnetic waves	Far-field/Radiative	Depending on distance, field oscillation frequency and energy harvester sensitivity, ranges from several meters to kilometers.	0.4% , above 18.2% and over 50% at -40dBm, -20dBm and -5dBm input power,respectively.	Radio communication, powering drones, wireless sensor and body networks, solar power satellites
Capacitive coupling	Near field/Non-radiative	up to several millimeters	low	smartcard technology, charging of hand-held devices, and power channeling in large scale ICs
Resonant inductive coupling	Near field/Non-radiative	few millimeters - few centimetres	Between 5.81% - 57.2%, when frequency varies from 16.2kHz to 508kHz	Radio Frequency Identification (RFID) tags, biomedical implants, electric vehicles, trains and buses, charging mobile phones
Resonant magnetic coupling	Near field/Non-radiative	few centimeters - few meters	For distances between 0.75m and 2.25m, ranges between 90% and 30% respectively	Plug-in Hybrid vehicle and mobile phone charging

Table 1.1: Wireless Power Control Techniques [1] [2]

1.2 Energy Harvesting

Energy harvesting, also called energy scavenging, is the process of capturing and storing energy from different available sources, which range from ambient ones like wind, solar, thermal or ambient radio communication signals etc to human-generated ones like body heat and finger motion. This activity has recently become attractive due to the proliferation of low power devices like sensors, body implants and mobile devices whose typical battery power sources require frequent recharging and may be difficult to replace when fully discharged either due to their remote, sensitive or mission-critical locations or simply inconvenient in the case of the latter. Table 1.2 details the characteristics of these ambient energy sources for comparison purposes. An energy source is adjudged *controllable* if it can be harnessed anytime for power harvesting purposes such that there is no need to predict its availability, whereas *non-controllable* sources which require prediction are harvested whenever available.

1.2.1 Energy Harvesting: Sources

Solar Energy

Despite being an uncontrollable source, the availability of solar energy can be forecast such that it can be harvested easily when present. Solar panels, made up of solar cells, exist in different forms and shapes - from gigantic arrays for powering whole municipalities to body-worn devices and sensors, and in fact solar is the most widely-applied energy harvesting technique in sensor-based energy-harvesting systems. The quantum of power that a solar panel generates depend on its cross-sectional area and the strength of the available light rays. Perhaps the most imaginative dimension into harvesting energy from the sun is the *solar-power satellite* or *satellite power system*

Energy Sources	Characteristics	Amount of available energy	Conversion efficiency	Amount of harvested energy	Energyvester	Harvester
Solar	Ambient, uncontrollable, predictable	100mW/cm2	15%	15mW/cm ² .	Solar cells.	
Wind	Ambient, uncontrollable, predictable	-	-	1200mWh/day	Anemometer.	
Vibrations in indoor environments	Ambient, uncontrollable, predictable	-	-	0.2mW/cm ² .	EM induction	
Radio/Microwaves	Ubiquitous availability	Up to tens of kW for microwaves [2]	0.4% , above 18.2% and over 50% at -40dBm, -20dBm and -5dBm input power, respectively.	0.4% , above 18.2% and over 50% at -40dBm, -20dBm and -5dBm input power, respectively.	Rectennas.	
Blood pressure	Passive human power, uncontrollable, unpredictable	0.93W	40%	0.37W	Micro-generator	
Breathing	Passive human power, uncontrollable, unpredictable	0.83W	50%	0.42W	Ratchet-Flywheel.	
Exhalation	Passive human power, uncontrollable, unpredictable	1W	40%	0.4W	Breath masks	
Finger motion	Piezoelectric, Fully controllable	19mW	11%	2.1mW	Piezoelectric	

Table 1.2: Energy Harvesting Sources [1] [2] [3]

(SPS) which was proposed by Peter Glacier [5] in 1968. It involves the transmission of solar power harvested from space and earth for use. The power is harvested by a satellite in orbit and then converted into microwaves to avoid absorption by clouds and rain in the intervening earth's atmosphere as it travels through it. SPS is advantageous because it assures continuous power generation and harvesting since there is no nighttime in the geostationary orbit, and also because higher amounts of energy can be harvested as the losses experienced by sunlight collected on earth are avoided due to conversion to microwaves in space as previously mentioned.

Wind Energy

Just like the sun, the wind is another uncontrollable but predictable ambient source of clean, green and renewable power source which is harnessed when wind turbines or rotors utilize exploit the power of airflow to drive generators which then generate electricity by following the principle of electromagnetic induction. It can be used as a compliment to conventional power sources to provide stable power supply to homes and townships. In comparison to other renewable sources, the problem with wind technology lies in the difficulty in miniaturizing its rotors, turbines, and generators. However, wind power continues to play an increasingly significant role in modern power generation, which is evidenced by the revelation that it was responsible for about 4% of worldwide energy usage in 2014 [6], and this is expected to increase in the coming years.

Piezoelectricity

Piezoelectric systems are those which apply the piezoelectric effect to generate electricity by various forms of exertion of force or pressure. They have been quite suc-

cessful in generating electricity through controllable and uncontrollable human mechanical body movements like finger, arm and leg motions and also blood pressure respectively. Piezoelectric technology has also been proposed for smart transportation systems. Generally, the amount of power harvested from such implementations is in the region of milliwatts and requires sustained and prolonged exercises to reach relatively significant levels. While signal successes have been achieved with the miniaturization of these sources, they have yet to find commercial success in low-power consumer electronic and mobile communications industry where energy harvesting technology is anticipated to be deployed in the nearest future, enabling users scattered over large geographical distances to renew their device power independently.

Radiowaves

Energy can also be harvested from ambient radiowaves which constitute the radiative component of electromagnetic radiation discussed in section 1.1. These transmissions exist in abundant proportions in the surrounding atmosphere as signals from broadcast and television stations and also wireless communication signals and are generally classified within the 3KHz - 300GHz frequency range, which in strict terms consists of radiowaves and microwaves, but is typically generalized as *radiowaves*. An energy harvesting receiver could be designed with an antenna or antennas which operate across a wide range of frequencies for example, presenting an opportunity to harvest as much energy as possible from all available transmitters in the surrounding environment. Significant success in energy harvesting with RF waves started being recorded within the low GHz (*microwave*) portion of the stated frequency range with William Brown's work on rectennas for capturing and rectifying signals at 2.45 GHz in the 1960s, and he eventually produced a rectenna which provided 40% and 50%

efficiency at 7W and 4W output power respectively in 1963. In 1964, he showed how a model tethered helicopter, using a rectenna, can harvest the power needed for its flight from microwaves beamed from the ground, and repeated the same feat for a free-flying chopper in 1968 [7].

While fairly substantial amounts of power were harvested from microwaves even after traversing long distances, the equipment used for such energy harvesting endeavours were quite bulky and expensive and could not be deployed on a large scale. However, the developments recorded in the low power consumer electronics and mobile communication industries in the last few decades has renewed interest in RF energy harvesting. The broadcast and far-field propagation characteristics of these portion of radiowaves make them an attractive option for powering several energy harvesting devices scattered over large geographical areas, particularly because they are capable of transmitting both energy and information within the same transmission.

Doubly Near-Far Problem However, such networks which are powered primarily by radio frequencies (termed RF-PCNs) have been shown to suffer from the *doubly near-far problem* [8] which involves remotely-located users harvesting much less amounts of energy in the DL from their associated transmitter stations and still having to transmit at higher power levels during UL information transmission. A number of techniques have been proposed in the literature for overcoming this phenomenon, these include:

- *Harvest-Then-Transmit(HTT)-based Common Throughput Maximization* [8]:

The HTT protocol employed in this work overcomes the doubly near-far problem with the use of an algorithm that adapts and optimizes the time allocation for wireless information transmission (WIT) based on the channel conditions of network users, ensuring that the common (equal) throughput calculated for all

users is optimized. It achieves that objective by allocating more WIT time to farther users while closer users get less time to transmit their information.

- *Harvest-then-Cooperate (HTC) - based user cooperation:* A user cooperative protocol is proposed in [9] for a two-user RF-PCN wherein a network user with better channel conditions in both uplink and downlink directions helps facilitate the transmission of the second user with relatively poor channel states to an HAP all to mitigate the doubly near-far problem. Specifically, the HAP performs downlink wireless energy transfer by broadcasting RF signals so that both users can harvest power, subsequently, the user closer to the HAP uses some of the time allocated to it and energy previously harvested to convey the information signals of the other user. Thereafter, it utilizes the remainder time and energy for its information transmission. This technique was employed in [10] where a canonical coalition game was used to model user cooperation in an energy-harvesting network, expressions for outage probability were provided and the stability of the grand coalition was also demonstrated.
- *Harvest-Then-Cooperate - based relay cooperation:* This aids communication in an RF-PCN network by using an intermediary node - a relay - to pass information or energy signals between transmitter and receiver nodes, and ultimately mitigate the effect of the doubly near-far problem. The work done in [11] incorporates a source node and a relay node, both of which perform energy harvesting energy in the downlink from a HAP and then cooperatively transmit information belonging to the source in the source uplink direction. Similarly, in [12], a source node, a relay node, and a destination node are considered where the relay node uses the energy that it harvests from a source for forwarding information transmitted by the latter to the destination. Time switching and

power-splitting protocols were also proposed for splitting WIT and WET at the relay.

- *Multi-Antenna Transmission with Energy Beamforming*: This approach combines the use of the HTT protocol, energy beamforming, and other multi-antenna techniques as applied in [13] and references therein to maximize energy reception at an energy harvester, especially those located far away from the HAP, so as to overcome the effect of the doubly near-far problem in an RF-PCN. Specifically, a multi-antenna HAP utilizes the HTT protocol to broadcast energy beams to energy harvesting users in the downlink, after which the users transmit their uplink information independently during the subsequent segment of the transmission block, using the energy previously harvested.

1.2.2 Energy Harvesting: Receiver Architecture

The figure below depicts the general schematic of a typical RF energy harvester. The grouping of functional blocks into energy harvesting and information processing circuits in the top and bottom sections, and their interconnection between the power management module and microcontroller, can be easily observed. The specific roles played by each block are explained in the following:

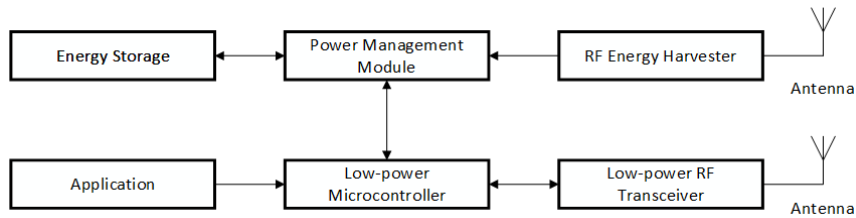


Figure 1.1: Energy Harvester Schematic [1]

For the energy harvesting line, the RF energy harvester is responsible for capturing the available RF power. This function block consists of a number of elements, first is the antenna/antennas on which the arriving oscillating electromagnetic waves impinge, inducing alternating current which is guided through to the receiver circuit. The next is the impedance matching circuit which is essentially a resonator circuit which functions at a set frequency to optimize wireless power transfer. The third element is the voltage multiplier which consists of diodes which rectify the alternating current from RF signals into DC current. The last is the capacitor which provides a temporary store of charge in situations where battery power is unavailable, like when they are being replaced. The power management module manages the exploitation of the received power using either of two self-explanatory mechanisms - *harvest-store-use* or *harvest-use* - where *use* refers to performing information transmission while the battery stores the harvested energy in the *harvest-store-use* mechanism.

At the information-processing segment, the low-power RF transceiver receives and transmits user information via its attached antenna/antenna array, the low-power microcontroller processes the data of the energy harvesting application which could be sensing, medical, mobile, healthcare-related to mention a few. In addition, the following techniques have also been proposed to facilitate seamless operation of the antenna/antenna array, energy harvesting and information processing circuits:

- *Time Switching* [14]: An antenna is connected to information transceiver and energy harvester circuitry and it switches periodically between them. Every transmission frame is partitioned into contiguous energy harvesting and data transmission time slots which are also orthogonal to each other.

- *Power Splitting* [14]: A power splitter is used to interconnect the antenna/antenna array to both circuits such that the incoming signal is separated into two different streams which are then channeled to the appropriate circuits.
- *Antenna Switching*: Is used in multi-antenna receivers, the array is separated into two groups, with either dedicated and connected to the information decoding and energy harvesting circuits. It is the same as time switching if there was just one antenna at the energy harvesting device.

1.2.3 Energy Harvesting for SBSs

Small cells base stations (SBSs) are miniature low-power versions of Macro Base Stations whose coverage area may range between 10 meters to a few kilometers, and are classified as femtocells, picocells or microcells in order of increasing service range. SBSs have been used to increase the coverage and capacity performance of modern wireless communication networks in schemes like traffic offloading from MBS service or network densification in areas with very dense phone usage, to mention a few. Due to their low-power consumption [15] and transmission attribute, SBSs are suitable candidates for RF energy harvesting as recommended in studies like the one conducted in [16].

1.3 Multi-Antenna Techniques

The desire for reliable, high bit-rate, and superior error performance communication which also meet the several QoS requirements of modern communication networks have led to the development of Multi-antenna techniques. These techniques overcome the multipath signal propagation and fading problems encountered in single-antenna

wireless systems by using multiple antenna elements at transmitters and receivers to create many transmission links between both ends, relying on the principle that the multipath fading experienced by each transmission link essentially becomes independent of the others when the separation distance between antenna elements at both transmitter and receiver is adequately large, and that the possibility of simultaneous degradation of all of such links is quite unlikely.

With the use of multiple antennas, these techniques essentially add a third dimension (spatial domain) to the time and frequency domains utilized in conventional single antenna systems to realize increased data rates, increased system capacity for multiple users and extended coverage without increasing channel bandwidth and transmission power. This is in contrast to single antenna systems where, given a particular channel bandwidth, achievable capacity increases in a logarithmic manner as the SNR increases by increasing the transmission power as given in Shannon's formula. In general, a multi-antenna system with M antennas at the transmitter end and N antennas at the receiver end experiences a linear capacity increase of approximately $\min(M, N)$, without the need for an additional increase in transmission power or bandwidth [17]. Generally, multi-antenna techniques are classified into the following:

- *Spatial multiplexing techniques*: these are used to communicate multiple independent data streams simultaneously over multiple transmit antenna elements. At the receiver, an interference elimination process is used to separate the independent data streams, an example of which is the Bell-Labs Layered Space-Time Architecture (BLAST) [17]. For a multi-antenna receiver, each antenna element receives all multiplexed data streams and would require spatial processing to extract each independent data stream by suppressing the interference from the

others. I consider Zero-forcing (ZF) and Minimum Mean Square Error (MMSE) linear receivers for this decoding purpose in this thesis.

While ZF decoders completely eliminate all the interference to a particular data stream from other streams and are ideal for noiseless environments, MMSE receivers are designed to maximize the receiver Signal-to-Noise (SNR) ratio for every data stream, where the noise element in this case incorporates both additive noise and interference from the accompanying data streams. A multi-antenna system that uses M antennas at the transmitter achieves an M -fold bit-rate increase (without additional power or bandwidth increase) over a single antenna transmitter due to spatial multiplexing. This bit-rate gain achieved is thus termed *spatial multiplexing gain*.

- *Spatial diversity techniques*: These enhance data transmission reliability by utilizing space-time coding to compensate for channel fading. Specifically, redundant signals of the same information sequence are transmitted out from the multi-antenna transmitter elements (spatial diversity) and combined at the receiver using proportionate techniques [17]. Spatial diversity outperforms channel coding used in single antenna systems because of the redundancy it employs in the additional spatial domain, and therefore results in *diversity and coding gains* [17] while maintaining the throughput levels achieved by such single-antenna systems.
- *Smart Antenna(Beamforming) techniques*: smart antennas utilize intelligent algorithms to acquire the spatial signature information of a target in a wireless network and use this to both design beamformers and situate the array beam on the intended target. Beamforming is the technique employed for creating the antenna or radiation pattern of an array, essentially performed by adding

the phases of the transmitted signals in a constructive manner such that their radiation is oriented in a predetermined desired direction while suppressing the antenna/radiation pattern for undesired ones.

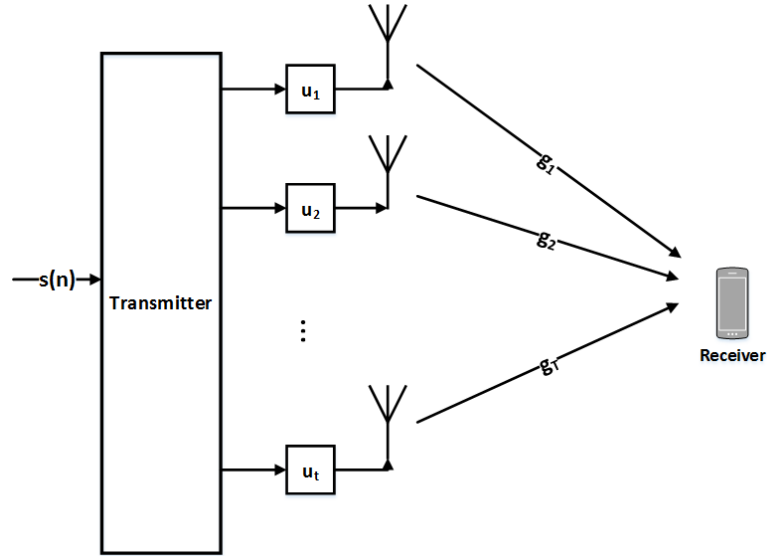


Figure 1.2: Transmit Beamforming

Beamforming techniques can be applied at both multi-antenna transmitters and receivers, as illustrated in Figs 1.2 and 1.3, resulting in *array and interference mitigation gains* [18], which pertain to SNR and SINR improvements over single-antenna systems respectively.

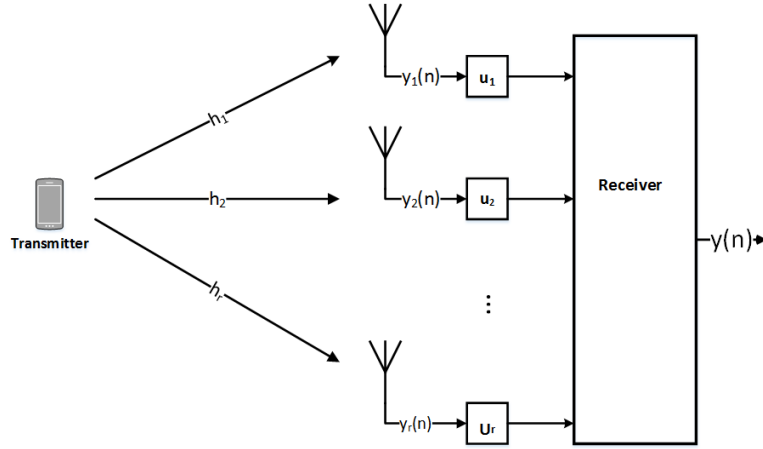


Figure 1.3: Receive Beamforming

Do note that $\mathbf{u} = [u_1, \dots, u_t]^T \in \mathbb{C}^{t \times 1}$ and $\mathbf{u} = [u_1, \dots, u_r]^T \in \mathbb{C}^{r \times 1}$ represent the transmit and receive beamformers in each figure.

1.4 Heterogeneous Networks

Due to the cost, capacity and coverage challenges encountered in homogeneous wireless cellular deployments, heterogeneous networks which incorporate a mixture of macro and low-power, lightweight small cell base stations are now being implemented in modern wireless communication networks as win-win solutions both to operators and network users. These SBSs could come in form of femtocells, picocells, microcells or even Wi-Fi access points and could be installed indoors or outdoors on poles, walls or even lamp posts. From the network operator perspective, the benefits of using small cell layers to underlay MBS service include extended coverage range by filling-in areas not serviced by macros, better network performance due to the offloading of traffic to SBS networks and cheaper site acquisition and maintenance costs due to the small footprint of SBSs. In addition, costs related to power consumption can be further reduced since SBSs can also be powered from RF-sources as discussed in

section 1.2.3. The benefits accruing to heterogeneous network users include increased bit-rates per unit area, much lower power transmissions due to the close proximity of their serving SBSs and improved cell-edge service.

1.5 Motivation

This thesis addresses crucial parameters of a futuristic telecommunications network, specifically power self-sustainability, coverage assurance for remote users, and rate-fairness. RF energy harvesting in wireless communication networks, including cellular, is a cost-effective and emerging practical approach to ensure power self-sufficiency for the billions of simultaneously connected and ubiquitously distributed devices accessing broadband services in modern-day networks, especially given the low-power, mobility and convenience-centric nature of their use which can not be provided by conventional one-to-one inductive or resonant coupling power transfer techniques.

Secondly, the provision of small cells in heterogeneous networks is a cost-effective way to extend coverage to otherwise disadvantaged indoor or cell-edge users, deliver higher throughputs for users in areas of high service demand like hotspots and assure much improved overall user experience and service quality to network users by handling offloaded traffic from overlaying macro tiers. In addition, the possibility of SBS energy harvesting [16] further provides an opportunity to make cellular communication networks green, environment-friendly and sustainable on the long-term. Lastly, meeting minimum QoS rare requirements in wireless communication networks is very important, therefore, this thesis also implements a scheme which ensures that users in the network, irrespective of their location, are guaranteed minimum SINR and rate levels, especially within the context of their energy-harvesting framework.

1.6 Problem definition

This thesis investigates minimum throughput maximization at both individual tier and overall network levels in a two tier heterogeneous wireless-powered communication network (WPCN) consisting of a multi-antenna HAP and an SBS at each tier which coordinate downlink energy beamforming and uplink information processing with their associated energy-harvesting users by the use of the Harvest-Then-Transit (HTT) protocol. This is so as to ensure that users in the network enjoy minimum QoS rate requirements, irrespective of their distance from their associated base stations, and especially because of the challenge posed by the doubly near-far problem phenomenon experienced by users in energy harvesting wireless communication networks where remote users have to transmit at higher power to achieve desired SINR levels despite being allocated the least amount of power to be harvested.

1.7 Related Work

Many policies, operational protocols and transmitter-receiver architectures have been proposed in WPCN literature to facilitate energy harvesting from RF signals. One of such is the *Harvest-Then-Transmit* (HTT) protocol [8], [13] where an RF source, typically called an HAP, first broadcasts wireless energy to network users who harvest it before transmitting their independent information to the HAP in the uplink in a TDMA scheme. In [8], common throughput maximization was proffered as a better metric to sum throughput optimization to counter the adverse effects the doubly near-far issue encountered in WPCNs. Since the system model had just one antenna at the HAP and user terminals, only the HTT time allocation variable was considered for optimizing the desired objective.

An interesting HTT-based WPCN system model was examined in [13] where a multi-antenna HAP and single-antenna receivers was considered, leading to the inclusion of downlink energy beamforming, power allocation, uplink information decoding and the HTT time allocation variables in the problem formulation. As done in [8], a fairness-guaranteeing utility function - the minimum data rate among network users - was maximized via a combined optimization of all the design variables previously mentioned.

Another technique, termed *Simultaneous Wireless Information and Power Transfer* (SWIPT), has been studied under single [19], [20] and multi-antenna [21], [22] systems and different receiver operating modes [14], [19], [20] and [21],. Generally, in SWIPT literature, some strategy is investigated to achieve desired trade-offs between achievable information rate and energy transfer either at the transmitter [14] or at the receiver [19] of such networks. In [20], resource allocation algorithm design for the maximization of the energy efficiency of data transmission was examined, whereas in [21], optimal resource allocation strategies in form of transmission information and energy covariances for maximizing harvested energy in secrecy MIMO systems were investigated. None of the previously listed considered the use of a hierarchical energy harvesting network system to increase the amount of energy harvested at distant users.

Energy harvesting in heterogeneous networks have also been considered in [16], [23], [24–27]. Based on their practical measurements, the authors of [16] recommend using SBSs to harvest energy from both the macrocell tier and also surrounding SBSs. [23] considers RF energy harvesting in an heterogeneous network where picocell base stations and dedicated Energy Transmission Towers (ETTs) are used to provide power for extending user uptime. The authors proposed an Integer Lin-

ear Programming (ILP) problem to maximize harvested energy while minimizing the number of active RF sources in the network. [24] and [25] consider stochastic energy arrivals in discussing power control policies for meeting predetermined objectives at both transmitter and receiver nodes of energy-harvesting networks. [24] incorporates a Central energy storage (CES) for harvesting, storing, and distributing energy to SBSs and applies game-theoretic and partial differential equation solution methodologies to obtain optimum SBS power control policies. [25] proposes content caching at SBS to reduce the load on backhaul links, formulates a discounted infinite horizon dynamic programming power control problem which they solve with a value iteration algorithm. Finally, [27] examines traffic offloading in a downlink heterogeneous network whose SBSs (termed and energy harvesting small cell access points (EH-SAPs)) only service users based on prioritized request and battery capacity. Based on the SBS power consumption model considered, network parameters including the rate coverage, network throughput, and energy efficiency are derived as functions of the macro and SBS densities, transmission powers, cell association biases, and energy harvesting capabilities.

1.8 Contribution

The contributions in the thesis are itemized below:

- I examine a two-tier energy harvesting WPCN system where a multi-antenna Hybrid Access Point and a Small Cell Base Station conduct WET and WIT with single-antenna network users.
- I implemented an adapted HTT protocol for the network that allows extended energy-harvesting duration for distant users and showed how energy beamforming leads to better power allocation to them.

- To ensure rate fairness at each tier, I maximized the minimum throughput of any one user, and then the total data rate a user across the whole network, subject to tier rate constraints.
- I elaborated on the alternating optimization algorithm on Table I of [13].
- I show that the optimal settings for the HTT time allocation variable in the first tier does not necessarily provide the best minimum throughput performance in the second, and that it also does not always guarantee the best total network throughput performance.

1.9 Organization of Thesis

The contents of this thesis are provided in three chapters, whose brief descriptions are itemized below:

- Chapter 2 presents mathematical preliminaries on the thesis. I discuss convex optimization and discuss the optimization tool used for formulating and solving the problems addressed in this work.
- In Chapter 3, I present my system model, assumptions, problem formulation and a solution methodology which employs an exhaustive alternating algorithm to obtain optimal parameters which satisfy the formulated optimization problem. I also present some simulation results.
- In Chapter 4, I provide a less-complex solution methodology to solve the formulated problem. I present more simulation results here, comparing the performance of both solution approaches and providing more insight.

- I bring the thesis to a conclusion in Chapter 5 by summarizing the work done and suggesting possible areas of work in the future.

Chapter 2

Mathematical Preliminaries

2.1 Mathematical Optimization

Mathematical optimization, also termed Mathematical programming or Nonlinear programming, could be generally described as the practice of finding the best solutions to mathematically conceptualized problems. In specific terms, it involves the identification, formulation and solution of a constrained problem often expressed in the form:

$$\min_{\mathbf{x}} f(\mathbf{x}) \tag{2.1}$$

subject to

$$g_j(\mathbf{x}) \leq 0, \quad j = 1, 2, \dots, m$$

$$h_j(\mathbf{x}) = 0, \quad j = 1, 2, \dots, r$$

where vector $\mathbf{x} = [x_1, x_2, \dots, x_n]^T \in \mathbb{R}^n$ is the design variable of the formulated problem, $f(\mathbf{x})$ is the objective or cost function, while $g_j(\mathbf{x})$ and $h_j(\mathbf{x})$ denote the inequality and equality constraint functions respectively. The constraints may also be collapsed the constraints into just one: $f_j(\mathbf{x}) \leq b_j \quad j = 1, \dots, m$, since the inequality is more

general than the equality constraint, and where b_j s are constraint limits. The optimal solution to equation 2.1 is the vector (\mathbf{x}^*) which has the least objective function value possible of all vectors that satisfy the stated constraints. The notation employed in this chapter is explained thus: $(\cdot)^T$ represents an array transpose, $(\cdot)^H$ represents conjugate transpose or Hermitian, $\text{rank}(\cdot)$ denotes the rank of a matrix, $\text{Tr}(\cdot)$ denotes the trace of a square matrix, $A \succeq 0$ and $A \succ 0$ imply that matrix A is positive semi-definite and positive-definite respectively, $|x|$ denotes the absolute value of a real or complex x while $\|x\|$ represents the Euclidean norm of complex vector $x \in \mathbb{R}^n$

2.1.1 Convex optimization: Introduction

Convex optimization is a subset of mathematical optimization in which the objective and constraint functions satisfy the inequality:

$$f_j(\alpha\mathbf{x} + \beta\mathbf{y}) \leq \alpha f_j(\mathbf{x}) + \beta f_j(\mathbf{y}) \quad (2.2)$$

where $\mathbf{y} = [y_1, y_2, \dots, y_n]^T \in \mathbb{R}^n$, $\alpha, \beta \in \mathbb{R}$, $\alpha, \beta \geq 0$ and $\alpha + \beta = 1$.

It is an interesting topic that has now been studied for about a century because of its increasing relevance to almost every field of human endeavour including finance, warfare, signal processing, and data analysis to mention a few. The advantage of identifying, formulating and/or converting problems to their convex optimization form is that such problems then be solved reliably, quickly and efficiently using any of many available solution methodologies. In addition, a locally optimal convex optimization solution, having satisfied tight optimality conditions, is also globally optimal, as verifiable by the duality theory. To provide a practical definition of a convex optimization problem, I need to define the following terminologies:

1. *Convex sets:* A set $\mathcal{S} \subset \mathbb{R}^n$ is defined as convex if the line segment joining any two points $x, y \in \mathcal{S}$ also lies in \mathcal{S} , that is:

$$\theta x + (1 - \theta)y \in \mathcal{S}, \quad \forall \theta \in [0, 1] \quad (2.3)$$

Examples of convex sets include the unit ball $\mathcal{S} = \{x \mid \|x\| \leq 1\}$, polyhedral sets, ellipsoids and so on. An important property of convex sets is that the intersection of any number of them is also convex.

2. *Convex functions:* A function $f(x) : \mathbb{R}^n \rightarrow \mathbb{R}$ is defined as convex over a convex set if, for any points $x, y \in \mathbb{R}^n$:

$$f(\theta x + (1 - \theta)y) \leq \theta f(x) + (1 - \theta)f(y), \quad \forall \theta \in [0, 1] \quad (2.4)$$

function $f(x)$ is said to be convex if the line segment between any x and y on the graph of $f(x)$ lies above or on the graph. Other properties of convex functions include:

- The first derivative $f'(x)$ or slope of $f(x)$ is non-decreasing as x increases.
- The second derivative $f''(x)$ of $f(x)$ is always nonnegative for all x in the interval.
- A local minimum of a convex function is also a global minimum.
- The Hessian of function f , $(\nabla^2 f)$ is $\succeq 0$ or $\succ 0$ for all values of x .

Examples of convex functions include x , $|x|$, $\|x\|$, \exp^x , x^2 , $x^T x$, $a^T x + b$, etc.

3. *Concave functions:* A function $f(x) : \mathbb{R}^n \rightarrow \mathbb{R}$ is concave over a convex set if, for any points $x, y \in \mathbb{R}^n$:

$$f((1 - \theta)x + \theta y) \geq (1 - \theta)f(x) + \theta f(y) \quad \forall \theta \in [0, 1] \quad (2.5)$$

This implies that $f(x)$ is concave if line segment between any x and y on the graph of $f(x)$ lies on or beneath the graph. A function f is concave if $-f$ is convex over the same set. $\nabla^2 f$ must be negative definite or negative semi-definite for all x for it to be adjudged concave. Examples of concave functions include \sqrt{x} , $\log x$, and the entropy function $-\sum_{i=1}^n x_i \log x_i$ (for $x > 0$).

There are some functions that are neither convex nor concave, an example is x^3 which is convex over $(-\infty, 0]$, concave over $[0, \infty)$ but cannot be said to be convex nor concave over \mathbb{R} .

2.1.2 *Convex optimization problem: Definition*

Based on the foregoing, a convex optimization problem involves the the minimization of a convex objective function or the maximization of a concave objective, subject to convex constraints, again, I consider eqt. (2.6) similar to (2.1) above:

$$\min \quad f_0(x) \quad (2.6)$$

subject to

$$f_i(x) \leq 0, \quad i = 1, 2, \dots, m$$

$$h_j(x) = 0, \quad j = 1, 2, \dots, r$$

$$x \in \mathcal{S}$$

where \mathcal{S} is the constraint set. With the objective functions and constraints described

earlier on, design variable x is *feasible* if $x \in \mathcal{S}$ and satisfies all constraints specified. For the optimization problem (2.6) to be termed *convex*, it must satisfy the following conditions: [28]:

- Functions $f_i(x)$ must be convex.
- Functions $h_j(x)$ must be of the form $a_j^T x + b_j$ for $a_j \in \mathbb{R}^n$ and $b_j \in \mathbb{R}$, i.e., they must be *affine*.
- \mathcal{S} must be convex.

If the *minimization* action on the objective is changed to a *maximization* and the direction of the inequality constraint is reversed, problem (2.6) still remains convex provided all $f_i(x)$ $i = 1, 2, \dots, m$ are concave. Any mathematical problem that does not satisfy the conditions listed above are *nonconvex*, which are generally difficult to solve, compared to their convex equivalents of which a large number (in terms of thousands of variables and constraints) can be quickly and reliably resolved.

Over the years, different theories, numerical algorithms and even software have been introduced to facilitate the resolution of convex optimization problems in different areas. One of such is the CVX [29] tool which was invented by Michael Grant and Stephen Boyd and is implemented in MATLAB. I utilized this tool extensively for solving my formulated optimization problems, and discuss its features in the next section.

2.2 CVX

CVX is a system for formulating and solving convex optimization problems which have been constructed in accordance to specialized rules invented by Michael Grant, Stephen Boyd and Yinyu Ye called *Disciplined Convex Programming* (DCP) [30].

2.2.1 Disciplined Convex Programming

Performing DCP involves working strictly within a number of guidelines to construct problems that one has decided ab-initio to be convex. These guidelines, called the *DCP ruleset*, are sufficient conditions for convexity of problem formulation, but are by no way absolute. Flouting any of their component rules will result in CVX rejecting the problem formulation, even if it is convex. The CVX distribution comes with a number of solvers, some of which are free and others require professional licenses for use. Problems which conform with the DCP guidelines are verified to be convex, translated to solvable form and subsequently solved. Although invented by the mentioned authors, DCP rules are based on basic convex analysis principles, therefore, disciplined convex programs are very similar in form to their natural mathematical forms. DCP allows enough flexibility to automate the analysis and solving of convex optimization problems if strictly adhered to.

As previously stated, CVX is implemented in MATLAB, and optimization problems are specified in it using MATLAB expressions. It supports a variety of problem types, including linear programs (LPs), quadratic programs (QPs), second-order cone programs (SOCPs), semidefinite programs (SDPs) and also non-convex problems like Mixed integer disciplined convex programs (MIDCPs) and geometric programming programs by appropriate DCP transformations and a special operating mode respectively. The rules govern the specification of objective functions and constraints, optimization problems, inequalities, expressions etc in CVX. In the table below, I provide a list of some of the DCP rules I adhered to in the process of writing this thesis. The items are by no means exhaustive, but I list them to provide an insight into how the CVX tool incorporates convex optimization in its solution process.

S/N	DCP Category	DCP Rule
1	Problem Definition	<ol style="list-style-type: none"> 1. Minimization problem: convex objective function, zero or more constraints. 2. Maximization problem: concave objective function, zero or more constraints. 3. Feasibility problem : one or more constraints and no objective.
2	Constraint usage	<ol style="list-style-type: none"> 1. Equality constraint (\equiv): used when LHS and RHS are affine. Either or both sides may be complex. Used to express set membership. 2. Less-than inequality constraint ($<$):Used when LHS is convex and RHS is concave. Both sides must be real. 3. Greater-than inequality constraint ($>$): Used when LHS is concave and Right Hand Side is convex. Both sides must be real. 4. Non-equality constraints (\sim): Non-convex, not allowed
3	Expression definition	<ol style="list-style-type: none"> 1. Constant expression: A Matlab expression that evaluates to a finite value. 2. Affine expression: a valid constant expression, a declared variable, a valid call to a function in the CVX atom library with an affine result, the sum or difference of affine expressions, the product of an affine expression and a constant. 3. Convex expression: a valid constant or affine expression, valid call to a function in the CVX atom library with a convex result, an affine scalar raised to a constant power $p \geq 1, p \neq 3, 5, 7, 9$, a convex scalar quadratic form, the sum of two or more convex expressions, the difference between a convex expression and a concave expression, the product of a convex expression and a nonnegative constant, the product of a concave expression and a nonpositive constant, the negation of a concave expression. 4. Concave expression: valid constant or affine expression, valid call to a function in the atom library with a concave result, a concave scalar raised to a power $p \in (0, 1)$, a concave scalar quadratic form, the sum of two or more concave expressions, the difference between a concave expression and a convex expression, the product of a concave expression and a nonnegative constant, the product of a convex expression and a nonpositive constant, the negation of a convex expression.
4	Function classification	<p>Are classified with respect to their curvature (constant, affine, convex, or concave) and monotonicity (nondecreasing, nonincreasing, or nonmonotonic). Functions with one argument are easily classified in terms of their curvature and monotonicity. For those with multiple arguments, monotonicity may be considered per argument, and curvature jointly.</p>
5	Function composition	<p>For a multi-argument function $f(x)$ of known curvature and monotonicity, each of its arguments must satisfy the following rules for $f(x)$ to be accepted by CVX and classified as convex:</p> <ul style="list-style-type: none"> • If the function is nondecreasing in an argument, that argument must be convex. • If the function is nonincreasing in an argument, that argument must be concave. <p>For a multi-argument function $f(x)$ of known curvature and monotonicity, each of its arguments must satisfy the following rules for $f(x)$ to be accepted by CVX and classified as concave:</p> <ul style="list-style-type: none"> • If the function is nondecreasing in an argument, that argument must be concave. • If the function is nonincreasing in an argument, that argument must be convex. • If the function is neither nondecreasing or nonincreasing in an argument, that argument must be affine.

Table 2.1: DCP Rules [30]

2.3 Array Math

In this thesis, I have worked extensively on vectors and matrices, and present some information about the work done on them in the following:

2.3.1 *Definitions*

1. **Array:** An array is an organized arrangement of numbers, usually expressed in terms of m rows and n columns (dimensions) of a matrix.
2. **Vector:** A vector is an element of a vector space \mathbb{R}^n . They are usually specified by the number of elements they contain, so an n -dimensional vector is usually called an n -vector.
3. **Matrix:** A matrix is a rectangular array of data entries in rows, columns and higher dimensions on which different operations can be performed. The most basic matrix type is the square matrix with m rows and n columns. Other matrix types include the diagonal matrix, identity matrix, orthogonal matrix, invertible matrix and so on.
4. **Eigenvalues and Eigenvectors:** A scalar λ and non-zero vector \mathbf{v} (of dimension n) which satisfy the linear equation $\mathbf{A}\mathbf{v} = \lambda\mathbf{v}$ are called the eigenvalue and eigenvector of square matrix \mathbf{A} of dimensions $n \times n$ respectively. The eigenvectors are the vectors that the linear transformation of matrix \mathbf{A} elongates or shrinks by an amount equal to the eigenvalue.
5. **Eigendecomposition:** Eigenvalue decomposition (EVD) is the factorization of a matrix into a simplified and most significant form without loss of generality by presenting it terms of its eigenvalues and eigenvectors. Square matrix \mathbf{A}

with linearly independent eigenvectors $q_i (i = 1, \dots, n)$ is factorized as: The eigendecomposition of matrix

$$\mathbf{A} = \mathbf{Q} \mathbf{\Lambda} \mathbf{Q}^{-1} \quad (2.7)$$

where:

- \mathbf{Q} : $n \times n$ matrix whose i -th column (q_i) is an eigenvector of \mathbf{A} .
- $\mathbf{\Lambda}$: A diagonal matrix whose diagonal elements ($\Lambda_{ii} = \lambda_i$) are eigenvalues corresponding to q_i .

2.3.2 Array Operations

1. Trace: For square matrices \mathbf{A} and \mathbf{B} ,

- $\text{Tr}(\mathbf{A}) = \sum A_{ii} = \sum_{i=1}^l \lambda_i$ (where $\lambda_i = i$ -th eigenvalue of \mathbf{A})
- $\text{Tr}(\mathbf{A}) = \text{Tr}(\mathbf{A}^T)$
- $\text{Tr}(\mathbf{A}^k) = \sum_{i=1}^l \lambda_i^k$
- $\text{Tr}(\mathbf{AB}) = \text{Tr}(\mathbf{BA}) \neq \text{Tr}(\mathbf{A}) * \text{Tr}(\mathbf{B})$
- $\text{Tr}(\mathbf{ABC}) = \text{Tr}(\mathbf{BCA}) = \text{Tr}(\mathbf{CAB}) \neq \text{Tr}(\mathbf{CBA})$ (cyclic rule).
- $\text{Tr}(\mathbf{A+B}) = \text{Tr}(\mathbf{A}) + \text{Tr}(\mathbf{B})$
- $\text{Tr}(c\mathbf{A}) = c\text{Tr}(\mathbf{A})$ where c is a constant.

2. Transpose and Hermittian

- $(\mathbf{AB})^T = \mathbf{B}^T \mathbf{A}^T$
- $(\mathbf{AB})^H = \mathbf{B}^H \mathbf{A}^H$

- $(\mathbf{AB})^{-1} = \mathbf{B}^{-1}\mathbf{A}^{-1}$
- $(\mathbf{A}^{-k}) = (\mathbf{A}^{-1})^k$
- $a^T a = \text{Tr}(aa^T)$, where a is an n -length vector.

3. Vector norms:

For any vector x

- $\|x\|_1 = \sum_i |x_i|$
- $\|x\|_2 = \sqrt{x^H x, x^T x}$
- $\|x\|_p = [\sum_i |x_i|^p]^{\frac{1}{p}}$

4. Matrix norms:

- $\|A\|_1 = \max_j \sum_i |A_{ij}|$
- $\|A\|_2 = \sqrt{\max \text{eig}(\mathbf{A}^H \mathbf{A})}$
- $\|A\|_p = (\max \|A_x\|_p)^{\frac{1}{p}}$
- $\|A\|_F = \sqrt{\sum_{ij} |A_{ij}|^2} = \sqrt{\text{Tr}(\mathbf{A}\mathbf{A})^H}$

Chapter 3

Adapted Harvest-Then-Transmit for a two-tier HetNet: MMSE decoders

3.1 System Model and Assumptions

I consider a heterogeneous WPCN consisting of a multi-antenna HAP and SBS, each operating at separate frequencies in two network tiers, K single-antenna HAP users (HAPUs) and S single-antenna small cell users (SCUs) denoted by $U_k, k = 1, \dots, K$ and $U_s, s = 1, \dots, S$, respectively. The HAP is assumed to be connected to a fixed power source and equipped with $M > 1$ antennas while the SBS, equipped with $B > 1$ antennas, is powered by both the energy it harvests from the HAP and some stand-by battery source (P_{batt}). It is also assumed that the U_k s and the U_s s are outfitted with rechargeable batteries with which they harvest energy and power their information transmission. For ease of analysis, each transmission block is assumed to be of unit length.

As depicted in Fig. 3.1, the HAP wirelessly broadcasts power during the first τ_1 fraction of transmission frame in the downlink (DL) direction to all energy-harvesting devices (HAPUs, SBS, and SCUs) in the network. Subsequently, the HAPUs transmit their information in the uplink (UL) to the HAP during the following $(1 - \tau_1)$ interval. At the second tier, the SBS harvests energy during τ_1 as previously mentioned, performs DL WET to the SCUs during τ_2 and finally processes UL WIT from its SCUs during the remainder $(1 - \tau_1 - \tau_2)$ interval. The energy harvesting efficiency coefficients at the users and SBS are denoted by ϵ and ς , respectively. DL information transmission between HAP/SBS and their users is not considered in this work.

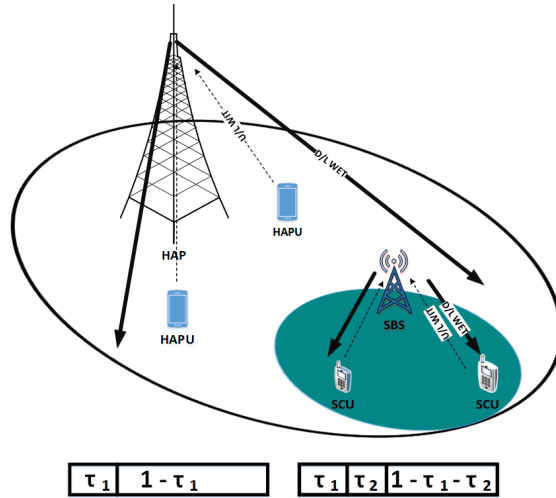


Figure 3.1: A two-tier HTT HetNet.

The HAP - HAPU complex channel vectors are modelled as $g_k \in \mathbb{C}^{M \times 1}$ and $h_k \in \mathbb{C}^{M \times 1}$, representing the DL and UL directions, respectively. $g_s \in \mathbb{C}^{B \times 1}$ and $h_s \in \mathbb{C}^{B \times 1}$ represent the SBS - SCU channels while $g_{sc} \in \mathbb{C}^{M \times 1}$ represents the DL WET channel from the HAP to the SCU and $G_b \in \mathbb{C}^{M \times B}$ represents the HAP to SBS MIMO channel matrix, all assumed to follow independent quasi-static flat fading.

3.1.1 DL WET to HAPUs

During the WET phase, the HAP with a total transmit power constraint P_{Tot} broadcasts energy wirelessly via l energy beams in the DL to the HAPUs, SBS, and SCUs. The broadcast transmit baseband energy signal is modelled as:

$$x = \sum_{i=1}^l v_i s_i^{dl} \quad (3.1)$$

where $v_i \in \mathbb{C}^{M \times 1}$ and s_i^{dl} represent the i th energy beam and its corresponding energy-conveying signal respectively, with $s_i^{dl} i.i.d \sim (0, 1)$ and $V = \{v_1, \dots, v_l\}$. Since the receiver noise at energy receivers is practically negligible [13], the received energy signal at each HAPU U_k is:

$$y_k = g_k^H x = g_k^H \sum_{i=1}^l v_i s_i^{dl} \quad k = 1, \dots, K \quad (3.2)$$

The energy harvested by each U_k is then given as:

$$E_k = \epsilon \tau_1 \sum_{i=1}^l |g_k^H v_i|^2 = \epsilon Tr(G_k \bar{S}) \quad k = 1, \dots, K \quad (3.3)$$

where $G_k = g_k g_k^H$, and $\bar{S} = \tau_1 S = \tau_1 \sum_{i=1}^l v_i v_i^H$. Assuming negligible circuit power consumption at each U_k , the mean transmit power available to it during its subsequent uplink transmission is:

$$\bar{P}_k(V, \tau_1) = \frac{\epsilon Tr(G_k \bar{S})}{1 - \tau_1}, \quad k = 1, \dots, k \quad (3.4)$$

3.1.2 DL WET to SBS and SCUs

The total power harvested by the SBS from the HAP during τ_1 is given as

$$Q = \varsigma\tau_1\mathbb{E}[\|G_b x\|^2] = \varsigma\tau_1\text{Tr}(G_b S G_b^H) \quad (3.5)$$

During the DL WET phase of duration τ_2 , the SBS broadcasts $b \leq B$ energy beams to the SCUs, with the energy signal denoted by

$$x_1 = \sum_{i=1}^b e_i s_i \quad (3.6)$$

with $e_i \in \mathbb{C}^{B \times 1}$ and s_i representing the i^{th} SBS energy beam and its corresponding energy-carrying signal, respectively, s_i being an i.i.d. random variable with zero mean and unit variance. In addition, $E = \{e_1, \dots, e_b\}$ and $S_s = \sum_{i=1}^b e_i e_i^H$.

The received energy signal at an SCU s after harvesting energy from the HAP and SBS is

$$y_s = g_{sc}^H x_0 + g_s^H x_1 = g_{sc}^H \sum_{i=1}^l v_i s_i^{dl} + g_s^H \sum_{i=1}^b e_i s_i, \quad s = 1, \dots, S \quad (3.7)$$

where s_i^{dl} is the energy-carrying signal of energy beam v_i from the HAP. The total energy harvested by each SCU from the HAP and SBS after τ_1 and τ_2 is thus given as

$$E_s = \epsilon[\tau_1 \sum_{i=1}^l |g_{sc}^H v_i|^2 + \tau_2 \sum_{i=1}^b |g_s^H e_i|^2], \quad s = 1, \dots, S. \quad (3.8)$$

The mean available power at SCU U_s during its succeeding uplink transmission period $1 - \tau_1 - \tau_2$ is thus given as

$$\bar{P}_s(E, \tau_1, \tau_2) = \frac{\epsilon[\text{Tr}(G_{sc}\bar{S}) + \text{Tr}(G_s\bar{S}_s)]}{1 - \tau_1 - \tau_2}, \quad s = 1, \dots, S \quad (3.9)$$

where $G_{sc} = g_{sc}g_{sc}^H$, $G_s = g_s g_s^H$, and $\bar{S}_s = \tau_2 \sum_{i=1}^b e_i e_i^H$ from (3.8). We also assume negligible power consumption at each U_s .

3.1.3 UL WIT Phase

After harvesting energy broadcast to them in the downlink, both tier users transmit information independently to their associated HAP and SBS respectively in the uplink. The UL SINR achieved by each user at the HAP or SBS is thus given as

$$\gamma_i = \frac{p_i u_i^H R_i u_i}{u_i^H \left(\sum_{j \neq i} p_j R_j + \sigma^2 I_{N_r} \right) u_i}, i = 1, \dots, K + S \quad (3.10)$$

where index i applies to either tier user such that p_i represents the UL transmit power of user U_i , $u_i \in \mathbb{C}^{N_r \times 1}$ is the beamformer used to decode U_i 's UL transmission and N_r denotes the number of receiver antennas at the HAP or SBS, $R_j = h_j h_j^H$ defines the channel covariance matrix and σ^2 denotes the additive white Gaussian noise (AWGN) power at each base station antenna element. Please note that the dot (\cdot) notation is sometimes used to distinguish tier 2 parameters from tier 1 parameters later in this work. Consequently, the achievable data rate of each user is given as

$$R_k = (1 - \tau_1) \log_2(1 + \gamma_k), \quad k = 1, \dots, K \quad (3.11)$$

$$R_s = (1 - \tau_1 - \tau_2) \log_2(1 + \gamma_s), \quad s = 1, \dots, S \quad (3.12)$$

for HAPU U_k and for SCU U_s , respectively.

3.2 Problem Formulation

To ensure rate fairness for users in the network, I maximize the minimum data rate of users in both tiers, resulting in two joint-parameter optimization formulations given below:

$$\max_{\{\tau_1, p_k, u_k, v_i\}} \min_{(1 \leq k \leq K)} R_k \quad (3.13)$$

subject to

$$\text{C1} \quad 0 \leq \tau_1 \leq 1$$

$$\text{C2} \quad p_k \leq \bar{P}_k, \forall k,$$

$$\text{C3} \quad \sum_{i=1}^l \|v_i\|^2 \leq P_{tot}$$

where p_k and u_k represent the transmit power allocation and uplink information decoder for U_k 's WIT transmission, respectively. The first constraint bounds the time allocation for τ_1 between 0 and 1, C2 ensures that U_k 's transmit power does not exceed the average available power that it had harvested in the preceding WET phase while C3 is the HAP transmission power constraint. After solving (3.13) and obtaining optimal values for the design variables, specifically τ_1 and S , I go ahead to solve the minimum rate maximization problem for the second tier, formulated as:

$$\max_{\{\tau_2, p_s, u_s, e_i\}} \min_{(1 \leq s \leq S)} R_s \quad (3.14)$$

subject to

$$\text{C1} \quad 0 \leq \tau_2 \leq 1 - \tau_1$$

$$\text{C2} \quad p_s \leq \bar{P}_s, \forall s,$$

$$\text{C3} \quad \sum_{i=1}^b \|e_i\|^2 \leq \varsigma \tau_1 \text{Tr}(G_b S G_b^H) + P_{batt}$$

where p_s and u_s are the uplink transmit power and information decoding vector for SCU U_s at tier 2. C1 above sets bounds for τ_2 , C2 constrains the transmission power

of the SCU so that it does not exceed the total power that it harvests from both the HAP and SBS. C3 ensures that the transmission power of the SBS does not exceed the sum of what it harvests from the HAP and the average available battery power P_{batt} .

The final problem definition is then to maximize the total network minimum throughput $R_{Tot} = R_k + R_s$, defined as:

$$\max \quad R_{Tot} \quad (3.15)$$

subject to

$$\text{C1:} \quad R_k \geq R_1, \quad \forall k$$

$$\text{C2:} \quad R_s \geq R_2, \quad \forall s$$

where R_1 and R_2 are constraints on the achieved data rates at each tier.

3.3 Solution Methodology

3.3.1 Background and Problem Simplification

To decode the independent uplink information stream transmissions from their associated users, I assume the use of beamformers u_i (where i applies to both k and s) at the HAP and SBS, and these are given as [31]:

$$u_i = \alpha_i \left(\sum_{k \neq i} p_k h_k h_k^H + \sigma^2 I_{N_r} \right)^{-1} h_i \quad i = 1, \dots, K + S \quad (3.16)$$

Where α_i is such that $\|u_i\|^2 = 1$. Due to the non-convexity of the formulated optimization problems (3.13) and (3.14), they cannot be solved with typical convex optimization techniques. I begin a relaxation process for these problems by initializing

a value for $\tau_1 = \tilde{\tau}_1$ and introducing a minimum SINR requirement constraint to (3.13), which results in the following:

$$\begin{aligned} & \max_{\{\gamma, p_k, u_k, v_i\}} \gamma & (3.17) \\ & \text{subject to} \\ \text{C1} \quad & \gamma_k(p_k, u_k) \geq \gamma, \quad \forall k, \\ \text{C2} \quad & p_k \leq \bar{P}_k, \quad \forall k, \\ \text{C3} \quad & \sum_{i=1}^l \|v_i\|^2 \leq P_{tot}. \end{aligned}$$

After solving for (3.13) above, requisite parameter values are substituted into (3.14), and then a similar problem relaxation (of fixing an initial value for τ_2 and common SINR requirement introduction) is carried out for the second tier formulation which converts (3.14) to:

$$\begin{aligned} & \max_{\{\dot{\gamma}, p_s, u_s, e_i\}} \dot{\gamma} & (3.18) \\ & \text{subject to} \\ \text{C1:} \quad & \gamma_s(p_s, u_s) \geq \dot{\gamma}, \quad \forall s \\ \text{C2:} \quad & p_s \leq \bar{P}_s, \quad \forall s \\ \text{C3:} \quad & \sum_{i=1}^b \|e_i\|^2 \leq \varsigma \tau_1 \text{Tr}(G_b S G_b^H) + P_{batt}. \end{aligned}$$

Equations (3.17) and (3.18) are SINR-balancing problem formulations, and the technique for solving them is explained next.

3.3.2 Perron Frobenius Theorem

Since most variables, utility functions and constraints encountered in wireless communication are usually of non-negative value, the Perron-Frobenius theory utilizes this

characteristic to resolve some non-convexity problems associated with them. The theory postulates states that every real square non-negative matrix $D_{(K \times K)}$ has a unique non-negative maximum eigenvalue or spectral radius $\rho(D)$ which in turn has a corresponding eigenvector whose elements are strictly non-negative. The theory also holds true if D were positive. The spectral radius is unique in that it is the only one of D 's eigenvalues whose corresponding eigenvector possesses the unique non-negative or positive attribute.

3.3.3 Equivalent Spectral Radius Minimization Formulation

In a direct application of the Perron-Frobenius theorem to WPCNs, it was demonstrated in [13], [32] and [33] that the desired balanced SINR level is obtained by calculating the inverse of the maximum spectral radius ρ (maximum non-negative eigenvalue) across all non-negative extended cross-talk matrices Φ_k of dimensions $(K + 1) \times (K + 1)$, constructed for each user U_k , with K being the total number of users. Considering tier 1, this translates to

$$\gamma(U, V) = \frac{1}{\max_{1 \leq k \leq K} \rho(\Phi_k(U, V))}. \quad (3.19)$$

where $U = \{u_1, u_2, \dots, u_K\}$. Furthermore, the optimal power allocation vector p which achieves the balanced SINR level has been given as the first K elements in the eigenvector corresponding to $\max_{1 \leq k \leq K} \rho(\Phi_k(U, V))$, which is typically of the form $\begin{pmatrix} p \\ 1 \end{pmatrix}$. The $K \times K$ non-negative matrix which specifies the uplink co-tier interference experienced by users is defined as:

$$[\Gamma(U)]_{i,k} = \begin{cases} u_i^H R_k u_i, & i \neq k \\ 0, & i = k \end{cases} \quad (3.20)$$

Next, I define a $K \times K$ diagonal matrix $\mathcal{Z}(U) = \text{diag} \left\{ \frac{1}{u_1^H R_1 u_1}, \dots, \frac{1}{u_K^H R_K u_K} \right\}$ and two K -length vectors $\sigma(U) = [(1 - \tilde{\tau}_1)\sigma^2 \|u_1\|^2, \dots, (1 - \tilde{\tau}_1)\sigma^2 \|u_K\|^2]^T$ and $w_k \in \mathbb{C}^{K \times 1}$, the latter being such that its k -th element is a 1 and others 0.

Finally, the desired $(K + 1) \times (K + 1)$ extended coupling matrix, constructed for each user k is defined as:

$$\Phi_k(U, V) = \begin{pmatrix} \mathcal{Z}(U)\Gamma(U) & \mathcal{Z}(U)\sigma(U) \\ \frac{1}{P_k(V, \tilde{\tau}_1)} w_k^T \mathcal{Z}(U)\Gamma(U) & \frac{1}{P_k(V, \tilde{\tau}_1)} w_k^T \mathcal{Z}(U)\sigma(U) \end{pmatrix}, \quad \forall k, \quad (3.21)$$

With the theorem expressed in (3.19), equation (3.17) is translated into the equivalent spectral radius minimization formulation below:

$$\min_{U, V} \quad \max_{1 \leq k \leq K} \rho(\Phi_k(U, V)) \quad (3.22)$$

$$\text{s.t.} \quad \sum_{i=1}^l \|v_i\|^2 \leq P_{tot}$$

Being dependent on the uplink receive decoding matrix U and the downlink energy beamforming matrix V , the objective in (3.22) is minimized by an alternating optimization process, that is, fixing the value of one variable and optimizing the other, and subsequently repeating the process until they both converge as described below:

$$\min_{(V)} \quad \max_{(1 \leq k \leq K)} \rho(\Phi_k(\tilde{U}, V)) \quad (3.23)$$

$$\text{s.t.} \quad \sum_{i=1}^l \|v_i\|^2 \leq P_{tot}$$

which fixes U and optimizes for V . By equating the objective above to a scalar $\theta > \rho(\Phi_k(\tilde{U}, V))$ and applying the extended coupling matrix $\Phi_k(\tilde{U}, V)$, a positive $(K + 1)$ -length vector q and θ above in the eigensystem equation $\Phi_k(\tilde{U}, V)q \leq \theta q$ [13],

it is easily seen how (3.23) becomes

$$\begin{aligned}
 & \min_{S, q, \theta} \theta & (3.24) \\
 & \text{subject to} \\
 \text{C1} \quad & \sum_{j=1}^K [X(\tilde{U})]_{i,j} \frac{q_j}{q_i \theta} + y_i(\tilde{U}) \frac{q_{K+1}}{q_i \theta} \leq 1, & 1 \leq k \leq K \\
 \text{C2} \quad & \sum_{j=1}^K [w_k^T X(\tilde{U})]_j \frac{q_j}{q_{K+1} \theta} + w_k^T y(\tilde{U}) \frac{1}{\theta} \leq \frac{\epsilon \tilde{\tau}_1 \text{Tr}(G_k S)}{1 - \tilde{\tau}_1}, & 1 \leq k \leq K \\
 \text{C3} \quad & \text{Tr}(S) \leq P_{tot} \\
 \text{C4} \quad & S \succeq 0
 \end{aligned}$$

Where $X(\tilde{U})$ and $y(\tilde{U})$ are the $(K \times K)$ and $(K \times 1)$ arrays $\mathcal{Z}(U)\Gamma(U)$ and $\mathcal{Z}(U)\sigma(U)$ from equation (3.21) respectively. Equation (3.24) is then solved with CVX to obtain the value for V . As previously stated, the second alternating optimization step fixes V and optimizes for U , that is:

$$\min_{(U)} \max_{(1 \leq k \leq K)} \rho(\Phi_k(U, \tilde{V})) \quad (3.25)$$

This step is implemented by an iterative update process of the MMSE beamformer U (3.16), after which consecutive ρ values are compared until they converge.

The whole process is executed in the alternating optimization solution algorithm which provides optimal U^* and V^* , $\max_{(1 \leq k \leq K)} \rho(\Phi_k(U^*, V^*)) = \rho^*$, and the optimal power allocation for the tier as the first K elements in the eigenvector corresponding to ρ^* . Subsequently, $\gamma(U, V)$ is obtained as the inverse of ρ^* (3.19), substituted into the objective in equation (3.13), and a one dimensional search is performed over τ_1 values to produce both optimal τ_1^* and the desired max-min R_k .

It should be noted that while equation (3.22) by itself is still non-convex, it has been proved in [13] and other references therein that the Perron-Frobenius-based alternating algorithm approach obtains the globally optimal values for the desired design variables. A similar procedure is employed to obtain max-min R_s at the SBS tier, with balanced SINR:

$$\dot{\gamma}(\mathbb{U}, E) = \frac{1}{\max_{1 \leq s \leq S} \rho(\Phi_s(\mathbb{U}, E))}. \quad (3.26)$$

where the matrix of uplink decoders $\mathbb{U} = \{u_1, u_2, \dots, u_S\}$. $S \times S$ non-negative arrays $\Gamma(\mathbb{U})$ and $\mathcal{Z}(\mathbb{U})$ are obtained as done in the previous formulation, while $\sigma(\mathbb{U}) = [(1 - \tilde{\tau}_1 - \tilde{\tau}_2)\sigma^2\|u_1\|^2, \dots, (1 - \tilde{\tau}_1 - \tilde{\tau}_2)\sigma^2\|u_S\|^2]^T$, $w_s \in \mathbb{C}^{S \times 1}$ and

$$\Phi_s(\mathbb{U}, E) = \begin{pmatrix} \mathcal{Z}(\mathbb{U})\Gamma(\mathbb{U}) & \mathcal{Z}(\mathbb{U})\sigma(\mathbb{U}) \\ \frac{w_s^T \mathcal{Z}(\mathbb{U})\Gamma(\mathbb{U})}{P_s(E, \tilde{\tau}_1, \tilde{\tau}_2)} & \frac{w_s^T \mathcal{Z}(\mathbb{U})\sigma(\mathbb{U})}{P_s(E, \tilde{\tau}_1, \tilde{\tau}_2)} \end{pmatrix}, \quad \forall s, \quad (3.27)$$

Equation (3.18) can then be translated to:

$$\min_{\mathbb{U}, E} \quad \max_{1 \leq s \leq S} \rho(\Phi_s(\mathbb{U}, E)) \quad (3.28)$$

$$\text{s.t.} \quad \sum_{i=1}^b \|e_i\|^2 \leq \varsigma \tilde{\tau}_1 \text{Tr}(G_b S G_b^H) + P_{batt}.$$

and commence the alternating parameter optimization procedure for \mathbb{U} and E . First, fix \mathbb{U} and update the energy beamforming matrix E :

$$\min_{(E)} \quad \max_{(1 \leq s \leq S)} \rho(\Phi_s(\tilde{\mathbb{U}}, E)) \quad (3.29)$$

$$\text{s.t.} \quad \sum_{i=1}^b \|e_i\|^2 \leq \varsigma \tilde{\tau}_1 \text{Tr}(G_b S G_b^H) + P_{batt}$$

which is equivalent to:

$$\min_{S_s, q, \theta} \theta \quad (3.30)$$

subject to

$$\begin{aligned} \text{C1} \quad & \sum_{j=1}^S [X(\tilde{\mathbb{U}})]_{i,j} \frac{q_j}{q_i \theta} + y_i(\tilde{\mathbb{U}}) \frac{q_{S+1}}{q_i \theta} \leq 1, \quad 1 \leq s \leq S \\ \text{C2} \quad & \sum_{j=1}^S [w_s^T X(\tilde{\mathbb{U}})]_j \frac{q_j}{q_{S+1} \theta} + w_s^T y(\tilde{\mathbb{U}}) \frac{1}{\theta} \leq \frac{\epsilon[\tilde{\tau}_1 \text{Tr}(G_{sc}S) + \tilde{\tau}_2 \text{Tr}(G_s S_s)]}{1 - \tilde{\tau}_1 - \tilde{\tau}_2}, \quad 1 \leq s \leq S \\ \text{C3} \quad & \text{Tr}(S_s) \leq \varsigma \tilde{\tau}_1 \text{Tr}(G_b S G_b^H) + P_{batt} \\ \text{C4} \quad & S_s \succeq 0 \end{aligned}$$

as demonstrated previously, and is solved with CVX. Note that for a particular initialized $\tilde{\tau}_2$ value, the optimal energy covariance S for every $\tilde{\tau}_1$ is also an input parameter into the SBS problem formulation since the SCUs also harvest energy from the HAPs during that time. The next step is to optimize for \mathbb{U} :

$$\min_{(\mathbb{U})} \max_{(1 \leq s \leq S)} \rho(\Phi_s(\mathbb{U}, \tilde{E})) \quad (3.31)$$

which is implemented by a recursive array update and comparison of successive $\rho(\Phi_s(\mathbb{U}, \tilde{E}))$ until convergence as previously stated.

(3.29) and (3.31) are iteratively executed until optimal \mathbb{U}^* , E^* , and eventually $\max_{(1 \leq s \leq S)} \rho(\Phi_s(\mathbb{U}^*, E^*))$ are obtained, with the optimal power allocation for the tier as the first S elements in the eigenvector corresponding to $\Phi_s(\mathbb{U}^*, E^*)$. For fixed $\tilde{\tau}_1$, $\dot{\gamma}(\mathbb{U}, E)$ is then obtained as the inverse of $\max_{(1 \leq s \leq S)} \rho\Phi_s(\mathbb{U}^*, E^*)$ in (3.26), substituted into the objective in equation (3.14), and a one dimensional search is performed over τ_2 values to produce both optimal τ_2^* and the desired max-min R_s . I present the algorithm that executes this process at both tiers of the network next:

Algorithm 1 Alternating Optimization Algorithm

Tier 1

- 1: Initiate feasible $V^{(1)}$, obtain p and update $U^{(1)}$ in (3.16)
- 2: **repeat**
- 3: $n = n + 1$
- 4: **for** $i = 1 : K$, where $i =$ user index, **do**
- 5: Obtain γ_i^n by substituting in (3.10).
- 6: Obtain $\rho(\Phi_i(V^{(1)}, U^{(1)})) = \rho_i^{(1)}$ and its eigenvector (p_i^1) .
- 7: Fix $V = V^{(1)}$, substitute p_i^1 in MMSE expression (3.16) to obtain $U_i^{(2)}$, then obtain $\rho_i^{(2)} = \rho(\Phi_i(V^{(1)}, U_i^{(2)}))$ and its eigenvector (p_i^2) .
- 8: If $\rho_i^{(2)} - \rho_i^{(1)} < \varepsilon$, $U_i^{(2)}$ is the optimal for user i for fixed $V^{(1)}$, else, reiterate till $U^{(n+1)}$ converges at $\rho_i^{(N)} = \rho(\Phi_i(V^{(1)}, U_i^{(N)}))$, note corresponding eigenvector (p_i^N)
- 9: p_i^N and $U_i^{(N)}$ are the optimal power and beamforming solutions, respectively, for user i .
- 10: **end for**
- 11: Of the K sets of power allocation vectors p_i^N obtained, one has elements which satisfy transmit power constraint $p_k \leq \bar{P}_k$. That $p_i^N = p^o$ and its corresponding $U_i^{(N)} = U^2$ are the optimal power allocation and uplink beamforming solutions respectively for the tier.
- 12: Substitute $U^{(2)}$ in (3.24) to update $V^{(2)}$.
- 13: With $U^{(2)}$ and p^o , obtain γ_i^{n+1} by substituting in (3.10).
- 14: **until** $\gamma_i^{n+1} - \gamma_i^n < \varepsilon$, ε being a small number preset tolerance value.
- 15: $\min_{(1 \leq i \leq K)} \gamma_i = \gamma^o =$ max-min SINR for the tier.
- 16: Substitute γ^o in (3.11) and perform one dimensional search over τ_1 to obtain optimal $\tau_1 = \tau^*$ and R_k .

Tier 2

- 17: **for all** τ_1 ($0 < \tau_1 < 1$) **do**
 - 18: Fix $\tau_1 = \tilde{\tau}_1$ and its corresponding energy covariance S from (3.24)
 - 19: Set $\tau_2 = \tilde{\tau}_2$ values ($0 < \tilde{\tau}_2 < 1 - \tilde{\tau}_1$) for every $\tilde{\tau}_1$.
 - 20: **for** $i = 1 : S$, where $i =$ user index, **do**
 - 21: Repeat steps 1–16 for all $\tilde{\tau}_2$, updating E in (3.30) to obtain R_s .
 - 22: **end for**
 - 23: **end for**
 - 24: Obtain $R_{Tot} = R_k + R_s$.
-

As indicated in step (24), the solution to the overall minimum network throughput maximization problem (4.7) is obtained by performing a search over all possible summations of R_k and R_s obtained via fixing values of τ_1 and exhaustively searching over corresponding τ_2 values on an incremental basis. The optimal R_k and R_s are the ones that maximize R_{Tot} .

3.4 Performance evaluation

Here, I provide the results obtained from implementing the alternating optimization technique detailed in Algorithm (1).

3.4.1 Simulation parameters

The parameter settings for the work done in this chapter are presented thus: I set $M = 6$ and $B = 4$ for the antenna elements at the HAP and SBS respectively, with $K = 3$ HAPUs and $S = 2$ SCUs, $P_{Tot} = 50\text{W}$ and $P_{batt} = 100\text{mW}$. Also, $\varsigma = 1$, $\epsilon = 0.6$, and $\sigma^2 = -50$ dBm. I consider spectral efficiency such that channel bandwidth is taken as 1, while R_1 and R_2 are given as 0.5 bps/Hz and 1 bps/Hz respectively. The free space attenuation in the network is given as follows:

$$\bar{L} = A_0 \left(\frac{d_i}{d_0} \right)^{-\alpha}, \quad i = 1, \dots, I \quad (3.32)$$

where $d_m = [10 \ 11 \ 12]$, $d_s = [2 \ 3]$ and $d_b = 15$ represent the HAP - HAPU, SBS to SCU and HAP - SBS distance values respectively, all in meters. $A_0 = 10^{-3}$, the reference distance $d_0 = 1$ m and path loss exponent $\alpha = 2$. The downlink channel

vectors are obtained from independent Rician distribution as:

$$g_i = \sqrt{\frac{K_R}{1 + K_R}} g_i^{LOS} + \sqrt{\frac{1}{1 + K_R}} g_i^{NLOS}, \quad \forall i \quad (3.33)$$

and assume channel reciprocity between UL and DL directions. Rician factor K_R is set to 3, while g_i^{LOS} and g_i^{NLOS} represent the line of sight and non line of sight (Rayleigh) channel realization fading components respectively, and are vectors of length M or B , depending on the transmitter concerned. The LOS component is modelled with the deterministic far-field uniform linear antenna array model as $g_i^{LOS} = [1, e^{j\theta_i}, e^{j2\theta_i}, \dots, e^{j(N_t-1)\theta_i}]^T$ where N_t is either M or B , $\theta_i = \frac{-2\pi d^{sp} \sin(\phi_i)}{\lambda}$, d^{sp} is the inter-antenna element spacing, λ is the carrier wavelength and ϕ is the angular orientation of the users to their associated HAP/SBS. In the simulations, I set $d^{sp} = \frac{\lambda}{2}$, $\phi_k = [-30^\circ \ 30^\circ \ 50^\circ]$ and $\phi_s = [50^\circ \ 70^\circ]$. The HAP to SBS MIMO channel matrix $G_b \in \mathbb{C}^{M \times B}$ follows independent quasi-static flat fading, with each entry being of an independent complex Gaussian distribution with zero mean and a covariance \bar{L} .

3.4.2 Numerical results

Fig. 3.2a shows how max-min R_k varies with time at the first tier. It can be seen that it initially increases with τ_1 due to the higher transmission power at the HAPUs from increased harvested energy in the preceding WET phase, peaking around $\tau_1 = 0.54s$. It was observed from simulations that the distance between HAPUs/SCUs and their associated transmitters and the transmit power at these coordinating stations have a direct influence on the time (τ) dedicated to DL WET. However, due to the assumed unit length of the transmission block, continuously increasing τ_1 results in a corresponding decrease in the amount of time available for the HAPUs to transmit in the uplink direction, thereby causing a reduction in the achieved max-min R_k , despite

the increase in harvested power. A similar trend can be observed in Fig. 3.2b which shows how R_s varies with τ_2 for different values of τ_1 . It can also be observed that, unlike the HAPUs, the SCUs do not need to harvest energy from the SBS for as long as the 1st tier HAPUs did before attaining their max-min rate. This is because they

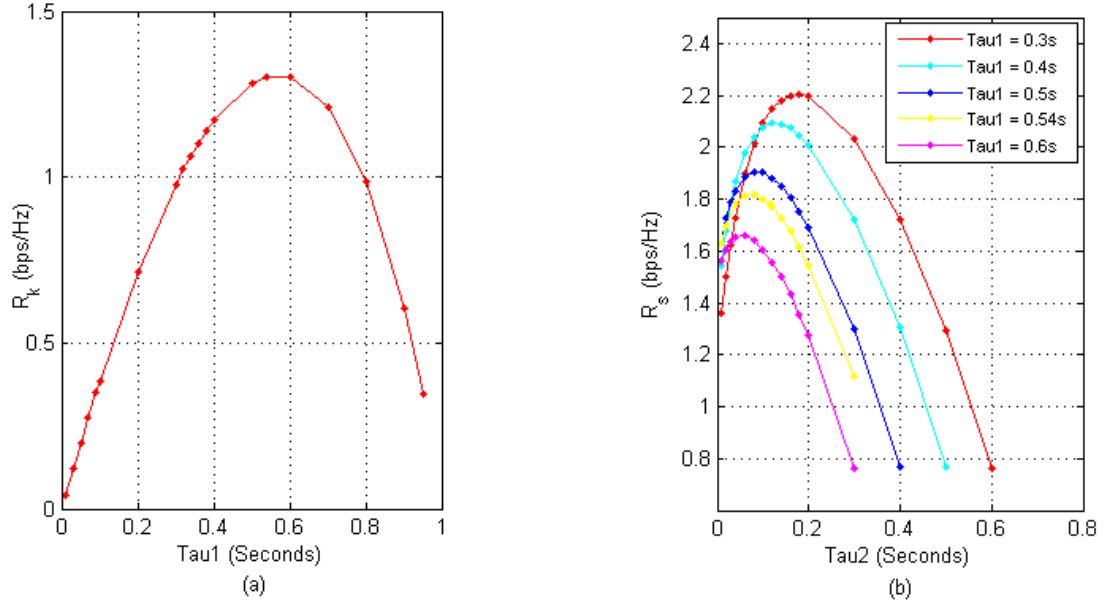


Figure 3.2: (a) R_k vs. τ_1 , (b) R_s vs. τ_2 for different τ_1 .

had started harvesting energy from the HAP during τ_1 . Perhaps the most interesting observation to be made here is that point here is that the $\tau_1 = 0.54$ s which yields (max-min) R_k in the first tier does not result in (max-min) R_s in the second, this verifies my assertion that the optimal HTT time allocated for energy harvesting in the first tier is not necessarily optimal for the second.

This observation is corroborated when I solve for equation (3.15) as illustrated in Fig. 3.3 below which presents 3D plots of R_{Tot} vs. τ_2 for different τ_1 values. It can be observed from Fig. 3.3b that the highest value for R_{Tot} is achieved at $\tau_1 = 0.4$ s, not $\tau_1 = 0.54$ s which optimizes for R_k for tier 1. This underscores the assertion that

optimal parameter setting for the first tier is not necessarily optimal for meeting the second and the network-wide rate requirements.

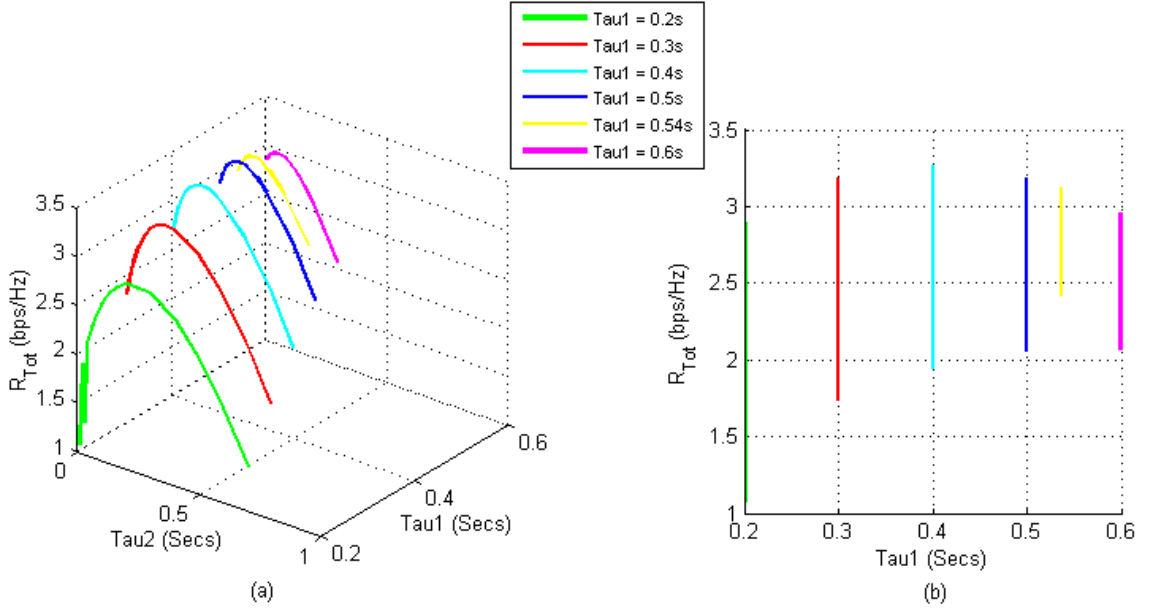


Figure 3.3: (a) 3D view of R_{Tot} vs. τ_1 for different τ_2 , (b) Different view of (a).

The next finding demonstrates the advantage of incorporating the additional spatial dimension via the use of multi-antenna transceivers to increase capacity in a multi-access system without increasing transmission power and bandwidth. In Fig 3.4a, the spatial multiplexing gain achieved can be seen to decrease as the number of HAP antennas decrease from 6 to 1, this is evidenced by the decrease in max-min R_k , and the same effect is generally noticed on R_{Tot} as shown in Fig 3.4b, although the reduction in total rate is not as steep as in 3.4a since the SBS also harvests energy not only from the HAP but also from P_{batt} and then transfers it to the SCUs which they use in the subsequent WIT phase. This further justifies the benefits of utilizing multi-antenna techniques in wireless communication systems.

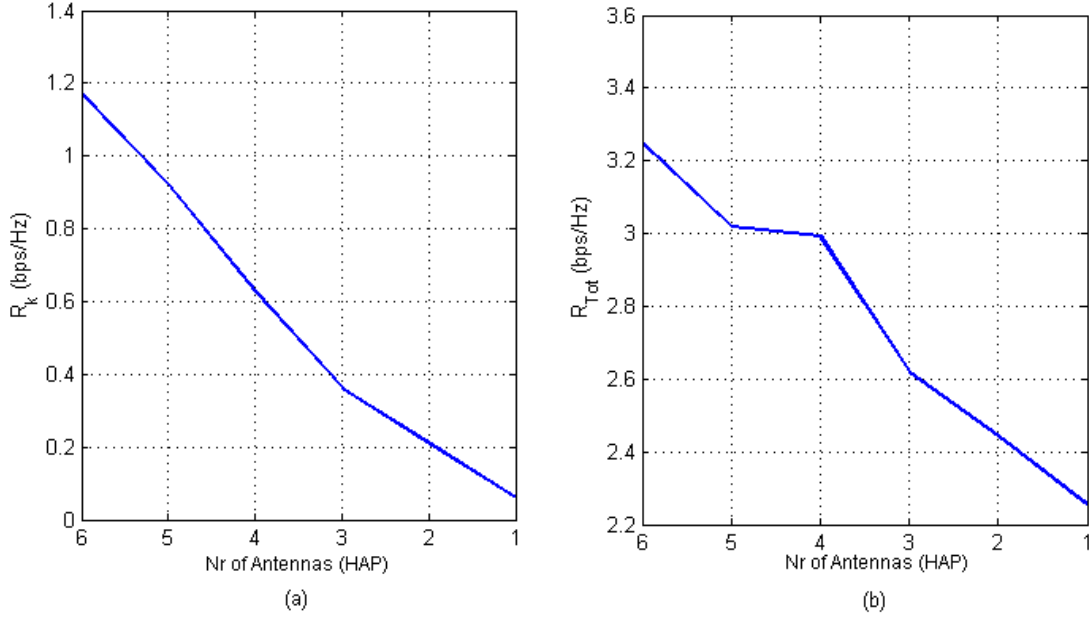


Figure 3.4: (a) R_k vs. Nr. of HAP Antennas (b) R_{Tot} vs. Nr. of HAP Antennas

Finally, I present Fig. 3.5a and Fig. 3.5b to illustrate how the alternating parameter optimization algorithm solution methodology ensures rate fairness in the network by balancing the SINRs of the HAPUs and SCUs in both tiers as τ_1 and τ_2 increase respectively. While it can be observed that the inverse spectral radius increases with τ as more time is allocated for harvesting energy in the downlink, this does not necessarily result in an increase in throughput as illustrated in Figs. 3.2a and 3.2b since increasing in τ_1 and τ_2 values result in a corresponding reduction in the time allocated for uplink information transmission in the adjoining segment of the HTT transmission block, and this time allocation is what ultimately determines the data rate as defined in equations (3.11) and 3.12.

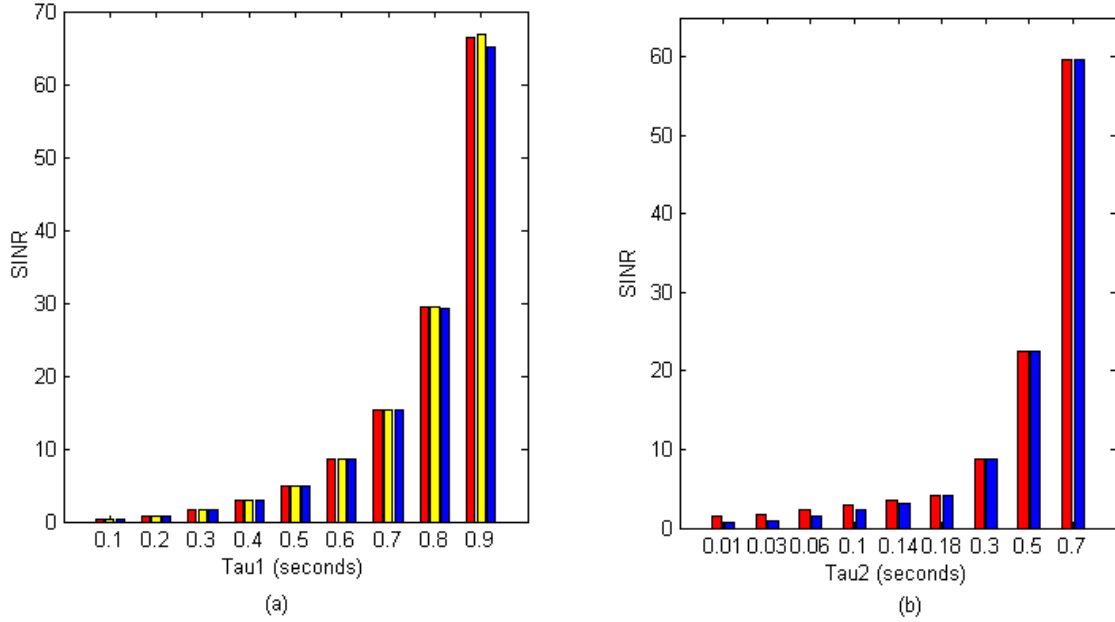


Figure 3.5: (a) HAP tier SINR balancing, (b) SBS tier SINR balancing.

3.5 Summary

In this chapter, I have presented the system model of a two-tier energy-harvesting heterogeneous network where a multi-antenna HAP overlaying a small-cell tier uses the HTT protocol to perform wireless power transfer to the HAP users (HAPUs), Small cell users (SCUs) and the SBS in the network. After the SBS performs WET in its own downlink, both the HAP and SBS also process the uplink information transmissions from their associated users. To ensure rate fairness at each in the network, I formulated multi-constraint optimization problems to maximize the minimum throughput within tier and overall network levels. I have solved the resulting non-convex optimization problems by first translating the original minimum rate maximization formulations into their spectral radius minimization equivalents and then applying an exhaustive alternating algorithm which exploits the Perron-Frobenius nonnegative matrix theory for parameter optimization. Finally, I have presented the

performance of the alternating algorithm solution methodology which, among other things, validated my assertion that the optimal time parameter setting in one tier of the network does not necessarily ensure that the desired objective for the second and overall network can be met.

Chapter 4

Adapted HTT for HetNets: Zero-Forcing decoders

4.1 Background

The exhaustive alternating algorithm problem provided in the previous chapter adopted the Perron-Frobenius non-negative matrix theory and a joint optimization of downlink energy beamformers, uplink information decoders, transmit power, and harvest-then-transmit time allocation for minimum-rate maximization in the network. In this chapter, I simplify the problem formulation and solution methodology by adopting Zero-forcing receivers for decoding uplink transmissions made to the SBS and the HAP, instead of the MMSE receivers previously used. It should be noted that MMSE and ZF are both linear receivers, but the former is more accurate as will be explained next. It is well known that the input-output model for MIMO AWGN channel with t and r antenna elements at the transmitter and receiver respectively is given as:

$$\mathbf{y} = \mathbf{H}\mathbf{x} + \mathbf{z} \quad (4.1)$$

where $\mathbf{y} \in \mathbb{C}^{r \times 1}$, $\mathbf{x} \in \mathbb{C}^{t \times 1}$, $H \in \mathbb{C}^{r \times t}$ and $\mathbf{z} \sim \mathcal{CN}(0, \sigma_z^2 \mathbf{I}_r)$.

Generally, a linear receiver applies a decoding array $\mathbf{U} \in \mathbb{C}^{r \times t}$ to the received signal \mathbf{y} for separating the signals from different data streams and then decodes them separately, that is:

$$\bar{\mathbf{y}} = \mathbf{U}\mathbf{y} = \mathbf{U}\mathbf{H}\mathbf{x} + \mathbf{U}\mathbf{z} \quad (4.2)$$

while MMSE receivers are designed such that \mathbf{U} minimizes the mean square error between the decoded signal and the transmitted signal ($\mathbb{E}[||\bar{\mathbf{y}} - \mathbf{x}||^2]$), ZF-receivers are designed to null inter-user interference, at the expense of losing some signal gain, with the result that decoder \mathbf{U} satisfies the relationship $\mathbf{U}\mathbf{H} = \mathbf{I}_t$, generally, the \mathbf{U} which satisfies this criterion is usually obtained as the pseudo-inverse of \mathbf{H} :

$$\mathbf{U} = \mathbf{H}^H(\mathbf{H}\mathbf{H}^H)^{-1} \quad (4.3)$$

MMSE receivers are the optimal linear decoders because, unlike their ZF equivalents, they do not simply eliminate the interference from all other data streams received alongside a particular user's transmission, they maximize the receiver SNR for each data stream, where the noise incorporates both the additive noise and the interference from all other data streams. In addition, MMSE receivers can process transmissions from any number of transceiver antenna elements while generally, for ZF receivers, the inequality $r \geq t$ must hold to satisfy the identity matrix output of channel matrices stated above. With the ZF decoder now given in closed form, the original problem

formulation is simplified. The signal-to-noise ratio for user i is thus given as:

$$\gamma_i = \frac{p_i |h_i^H u_i|^2}{\sigma^2} = \frac{p_i \tilde{h}_i}{\sigma^2}, \quad i = 1, \dots, K + S \quad (4.4)$$

where index i applies to either tier user as previously stated such that p_i represents the UL transmit power of user U_i , $u_i \in \mathbb{C}^{N_r \times 1}$ is the ZF-beamformer used to decode U_i 's UL transmission and N_r denotes the number of receiver antennas at the HAP or SBS as previously stated, and \tilde{h}_i captures the uplink channel and beamformer product for user i .

4.2 Problem Formulation

Consequently, I substitute the SNR expression (4.4) and insert a common rate constraint on all HAPUs into (3.13) to obtain the equivalent max-min data rate optimization problem for the HAPUs as:

$$\max_{\{\tau_1, \bar{p}_k, \bar{S}, R_k\}} R_k \quad (4.5)$$

subject to

$$\begin{aligned} \text{C1} \quad & 0 < \tau_1 < 1 \\ \text{C2} \quad & (1 - \tau_1) \log_2 \left(1 + \frac{\bar{p}_k \tilde{h}_k}{(1 - \tau_1) \sigma^2} \right) \geq R_k \\ \text{C3} \quad & \bar{p}_k \leq \epsilon \text{Tr}(G_k \bar{S}), \quad \forall k, \\ \text{C4} \quad & \text{Tr}(\bar{S}) \leq \tau_1 P_{tot} \end{aligned}$$

C1 sets the bounds for τ_1 , C2 is the common minimum rate constraint on all HAPUs, C3 sets the uplink transmission power constraint at each HAPU and C4 limits the downlink transmission power at the HAPU. Note that $\bar{p}_k = p_k(1 - \tau_1)$, this minimum-rate maximization problem as formulated can then be solved with CVX [29] to obtain

τ_1 , the optimal power allocation solution $p = [p_1, \dots, p_k]$, the optimal energy beamforming matrix $S = \bar{S}/\tau_1$ and the max-min rate R_k .

With the outputs from solving (4.5) above, I proceed to solve for the SBS tier, where the minimum rate maximization for U_s is formulated to be:

$$\max_{\{\tau_2, \bar{p}_s, \bar{S}_s, R_s\}} R_s \quad (4.6)$$

subject to

$$\begin{aligned} \text{C1} \quad & 0 < \tau_2 < 1 - \tau_1 \\ \text{C2} \quad & (1 - \tau_1 - \tau_2) \log_2 \left(1 + \frac{\bar{p}_s \bar{h}_s}{(1 - \tau_1 - \tau_2) \sigma^2} \right) \geq R_s \\ \text{C3} \quad & \bar{p}_s \leq \epsilon [Tr(G_{sc} \bar{S}) + Tr(G_s \bar{S}_s)], \quad \forall s, \\ \text{C4} \quad & Tr(\bar{S}_s) \leq \tau_2 (\varsigma Tr(G_b \bar{S} G_b^H) + P_{batt}) \end{aligned}$$

where $\bar{p}_s = p_s(1 - \tau_1 - \tau_2)$, in addition, C1 sets the bounds for τ_2 , C2 is the common data rate requirement at tier 2, C3 limits the transmit power at the SCU to what it harvests from the HAP and SBS while C4 limits the SBS' transmit power to what it harvests from the HAP and the battery power available to it. Also, equation (4.6) as formulated can also be solved with the use of CVX [29] to obtain optimal values for the design variables τ_2 , $S_s = \bar{S}_s/\tau_2$ and $p_s = \bar{p}_s/(1 - \tau_1 - \tau_2)$.

After solving for R_k and R_s , the overall network minimum rate optimization can then be performed by performing a search over all possible summations of R_k and R_s obtained via fixing values of τ_1 and exhaustively searching over corresponding τ_2 values on an incremental basis.

$$\max \quad R_{Tot} \tag{4.7}$$

subject to

$$\text{C1: } R_k \geq R_1, \quad \forall k$$

$$\text{C2: } R_s \geq R_2, \quad \forall s$$

Where optimal R_k and R_s are the ones that maximize R_{Tot} as previously mentioned, and R_1 and R_2 are constraints on the achieved data rates at each tier.

4.3 Performance evaluation

Employing the same simulation parameters used in the alternating optimization solution, I present simulation results in this segment to demonstrate the performance of the ZF-solution methodology and compare it with the optimal. I start by looking at how the doubly near-far problem is overcome in the network as illustrated in Fig. 4.1 below. It can be seen that users at the farthest location (HAPU 3 and SCU 2), which could be cell-edge users of a real network, are allocated the highest amount of power with time, thereby ensuring that they consistently have enough power to transmit in the uplink after harvesting energy in the preceding downlink WET phase.

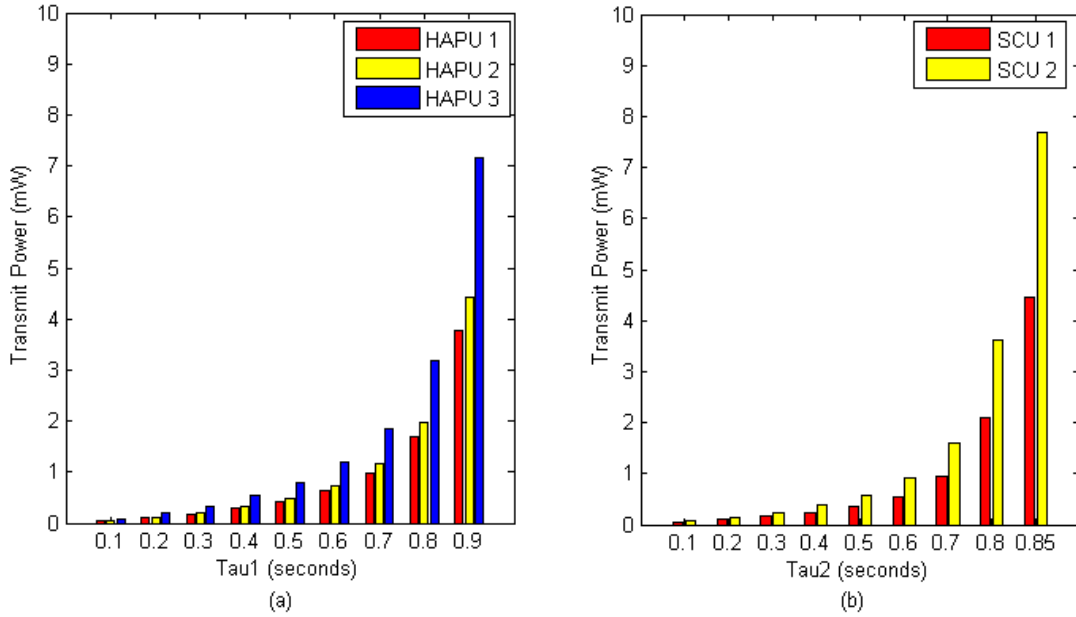


Figure 4.1: (a) Tier 1 power allocation , (b) Tier 2 power allocation, $\tau_1 = 0.1$.

The second finding, illustrated in Fig 4.2 below, compares the max-min R_k and max-min R_{Tot} performance of the two solution methodologies considered. It can be seen in Fig 4.2a that the iterative algorithm solution achieves a much higher minimum

throughput than its ZF solution equivalent, exceeding it by over 1 bps/Hz at its peak. This is due to the more accurate beamformer and power allocation values resulting from the exhaustive alternating parameter optimization process. The same deduction can be made from the plots of the maximized minimum network throughput with τ_2 illustrated in Fig 4.2b where the alternating optimization-based solution produces a maximized minimum R_{Tot} of 3.3 bps/Hz while the ZF decoders provide 1.9 bps/Hz peak R_{Tot} .

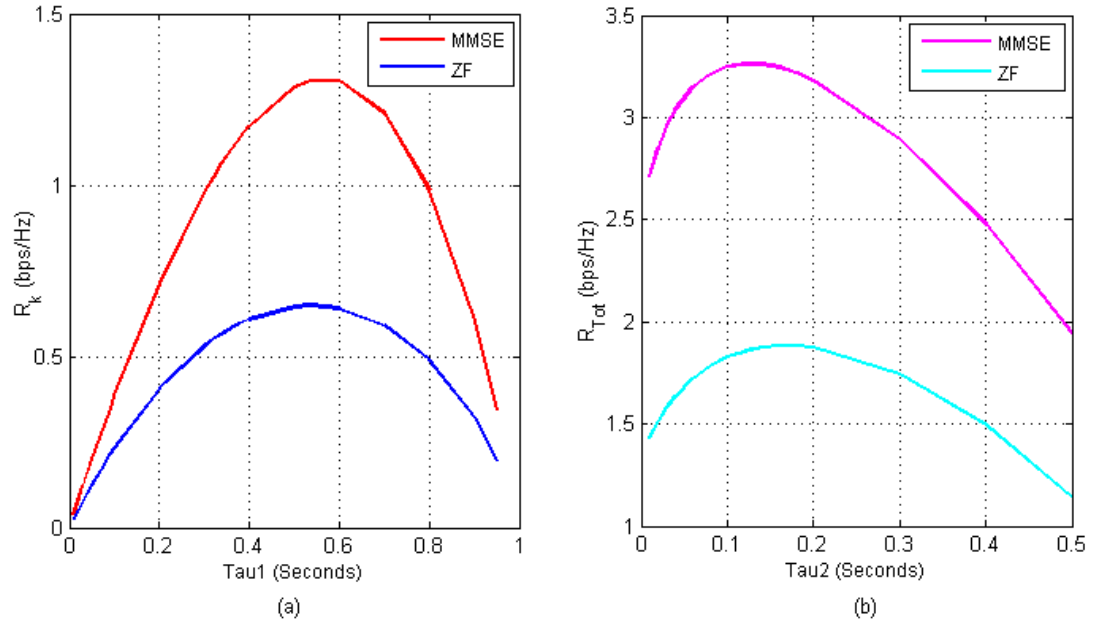


Figure 4.2: (a) R_k vs τ_1 :MMSE vs ZF , (b) R_{Tot} vs τ_2 , $\tau_1 = 0.4s$.

Finally, I present the performance of the solution methodologies under different HAP transmit power levels in Fig 4.3 which plots R_k against different HAP transmit power levels P_{Tot} for both the alternating optimization algorithm and ZF-beamformer solution. It can be seen that, with both approaches, the higher the transmit power, the higher the max-min R_k achieved by the HAPUs. Again, the alternating algorithm solution achieves higher minimum rate levels than its zero-forcing equivalent for the

same reasons that had been mentioned previously in this thesis.

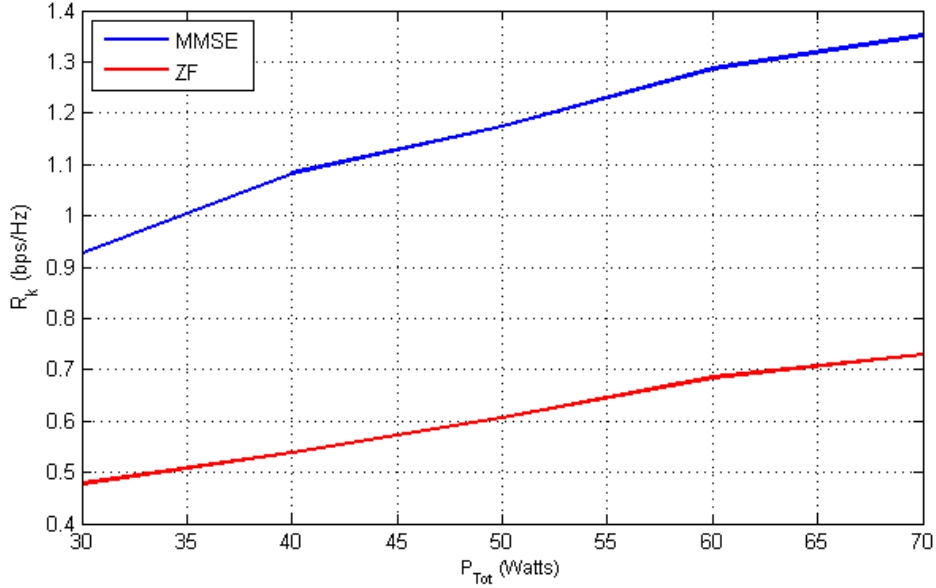


Figure 4.3: R_k vs P_{Tot} : MMSE vs ZF

4.4 Summary

I have reduced the complexity of the solution to the network minimum throughput maximization problem as formulated by utilizing closed form Zero-forcing decoders, thus leaving us with just three design variables as against four that were jointly optimized in the solution methodology proposed in the previous chapter. I have applied disciplined convex programming rules in reformulating and subsequently solving the multi-constraint optimization problem. Finally, I have presented findings to illustrate how, among other things, the alternating parameter optimization approach produces better max-min throughput performance in the network than the less-complex zero-forcing approach.

Chapter 5

Conclusion and Future Work

5.1 Conclusion

In this thesis, I have investigated minimum rate maximization in two tiers of a heterogeneous wireless communication network which utilizes the HTT protocol for energy harvesting. A multi-constraint optimization problem was formulated for the specified objective and solution methodologies were presented in 2 chapters. In Chapter 3, an exhaustive alternating algorithm which incorporates the Perron-Frobenius non-negative matrix theory for joint optimization of downlink energy beamformers, uplink information decoders and user transmit power was proposed to solve minimum rate maximization at each tier, before finally obtaining the overall network minimum throughput via a one dimensional search over HTT time allocation values.

In Chapter 4, I applied a closed-form uplink information transmission decoder in the problem formulation, thereby reducing the number of design variables in the problem formulation by one, and subsequently applied disciplined convex programming rules to solve the designed problem. Across both chapters, I presented the performance of the solution methodologies in terms of power allocation for ensuring rate

fairness in the network, SINR balancing, advantages of using multiple antennas, and ultimately showed that the tier and rate performance of the alternating optimization algorithm solution methodology betters that of the simplified zero-forcing approach.

5.2 Future Work

The following are possible areas for improving on the work done in this thesis:

- The positioning of users could be made to follow some random distribution as against the deterministic uniform linear array (ULA) approach employed here.
- Using the same frequency for WIT transmissions at the HAP and SBS may be considered. This will introduce co-channel interference across both tiers, and a new channel model will have to be used as the ULA model will not suffice in that case, but may lead to interesting results.
- The aspect of association may also be considered, a system model that allows the SCU and HAPU to associate with either HAP or SBS based on a number of parameters like received signal strength, inter-transceiver distance, or available throughput will also generate interesting results.
- In the place of the HTT protocol, it will be interesting to see the throughput performance results of a system model that adopts the SWIPT technique, as users will perform WET and WIT at the same time. While challenges have been highlighted in the literature about the practicability of this because of the different receiver sensitivities for information decoding and energy harvesting (-60 dBm and -10 dBm) respectively, achievable capacity from such a model may be higher from the one described here as users will be transmitting information for the whole length of the transmission frame.

Bibliography

- [1] X. Lu, P. Wang, D. Niyato, D. I. Kim, and Z. Han, “Wireless networks with rf energy harvesting: A contemporary survey,” *Communications Surveys & Tutorials, IEEE*, vol. 17, no. 2, pp. 757–789, 2015.
- [2] S. S. Valtchev, E. N. Baikova, and L. R. Jorge, “Electromagnetic field as the wireless transporter of energy,” *Facta universitatis-series: Electronics and Energetics*, vol. 25, no. 3, pp. 171–181, 2012.
- [3] S. Sudevalayam and P. Kulkarni, “Energy harvesting sensor nodes: Survey and implications,” *Communications Surveys & Tutorials, IEEE*, vol. 13, no. 3, pp. 443–461, 2011.
- [4] J. I. Agbinya, *Wireless power transfer*. River Publishers, 2012.
- [5] P. E. Glaser, “Power from the sun: its future,” *Science*, vol. 162, no. 3856, pp. 857–861, 1968.
- [6] S. Pereira, P. Ferreira, and A. Vaz, “Short-term electricity planning with increase wind capacity,” *Energy*, vol. 69, pp. 12–22, 2014.
- [7] W. C. Brown, “The history of power transmission by radio waves,” *IEEE Transactions on Microwave Theory and Techniques*, vol. 32, no. 9, pp. 1230–1242, Sep 1984.

- [8] H. Ju and R. Zhang, “Throughput maximization in wireless powered communication networks,” *IEEE Transactions on Wireless Communications*, vol. 13, no. 1, pp. 418–428, January 2014.
- [9] —, “User cooperation in wireless powered communication networks,” in *Global Communications Conference (GLOBECOM), 2014 IEEE*. IEEE, 2014, pp. 1430–1435.
- [10] Z. Ding and H. V. Poor, “Cooperative energy harvesting networks with spatially random users,” *Signal Processing Letters, IEEE*, vol. 20, no. 12, pp. 1211–1214, 2013.
- [11] H. Chen, Y. Li, J. L. Rebelatto, B. F. Ucha-Filho, and B. Vucetic, “Harvest-then-cooperate: Wireless-powered cooperative communications,” *IEEE Transactions on Signal Processing*, vol. 63, no. 7, pp. 1700–1711, April 2015.
- [12] A. A. Nasir, X. Zhou, S. Durrani, and R. A. Kennedy, “Relaying protocols for wireless energy harvesting and information processing,” *IEEE Transactions on Wireless Communications*, vol. 12, no. 7, pp. 3622–3636, July 2013.
- [13] L. Liu, R. Zhang, and K. C. Chua, “Multi-antenna wireless powered communication with energy beamforming,” *IEEE Transactions on Communications*, vol. 62, no. 12, pp. 4349–4361, Dec 2014.
- [14] R. Zhang and C. K. Ho, “Mimo broadcasting for simultaneous wireless information and power transfer,” *IEEE Transactions on Wireless Communications*, vol. 12, no. 5, pp. 1989–2001, May 2013.
- [15] M. Deruyck, D. D. Vulder, W. Joseph, and L. Martens, “Modelling the power consumption in femtocell networks,” in *Wireless Communications and Networking Conference Workshops (WCNCW), 2012 IEEE*, April 2012, pp. 30–35.
- [16] D. Muirhead, M. Imran, and T. Brown, “Energy harvesting opportunities and applicability in two tier heterogeneous networks,” in *Antennas and Propagation Conference (LAPC), 2014 Loughborough*, Nov 2014, pp. 487–490.

- [17] J. Mietzner, R. Schober, L. Lampe, W. H. Gerstacker, and P. A. Hoeher, “Multiple-antenna techniques for wireless communications - a comprehensive literature survey,” *IEEE Communications Surveys Tutorials*, vol. 11, no. 2, pp. 87–105, Second 2009.
- [18] R. Zhang, “Adaptive and spatial based wireless communications,” <https://www.ece.nus.edu.sg/stfpage/elezhang/>, accessed: 2016-06-10.
- [19] L. Liu, R. Zhang, and K. C. Chua, “Wireless information transfer with opportunistic energy harvesting,” *IEEE Transactions on Wireless Communications*, vol. 12, no. 1, pp. 288–300, January 2013.
- [20] D. W. K. Ng, E. S. Lo, and R. Schober, “Wireless information and power transfer: Energy efficiency optimization in ofdma systems,” *IEEE Transactions on Wireless Communications*, vol. 12, no. 12, pp. 6352–6370, December 2013.
- [21] W. Wu, X. Zhang, and B. Wang, “Energy harvesting in secure MIMO systems,” *CoRR*, vol. abs/1601.03468, 2016. [Online]. Available: <http://arxiv.org/abs/1601.03468>
- [22] K. Huang and E. Larsson, “Simultaneous information and power transfer for broadband wireless systems,” *IEEE Transactions on Signal Processing*, vol. 61, no. 23, pp. 5972–5986, Dec 2013.
- [23] M. Erol-Kantarci and H. T. Mouftah, “Radio-frequency-based wireless energy transfer in lte-a heterogeneous networks,” in *Computers and Communication (ISCC), 2014 IEEE Symposium on*, June 2014, pp. 1–6.
- [24] T. K. Thuc, E. Hossain, and H. Tabassum, “Downlink power control in two-tier cellular networks with energy-harvesting small cells as stochastic games,” *CoRR*, vol. abs/1510.07932, 2015. [Online]. Available: <http://arxiv.org/abs/1510.07932>
- [25] A. Kumar and W. Saad, “On the tradeoff between energy harvesting and caching in wireless networks,” *CoRR*, vol. abs/1505.06252, 2015. [Online]. Available: <http://arxiv.org/abs/1505.06252>

- [26] S. Zhang, N. Zhang, S. Zhou, J. Gong, Z. Niu, and X. Shen, “Energy-aware traffic offloading for green heterogeneous networks,” *CoRR*, vol. abs/1601.03505, 2016. [Online]. Available: <http://arxiv.org/abs/1601.03505>
- [27] P. S. Yu, J. Lee, T. Q. S. Quek, and Y. W. P. Hong, “Traffic offloading in heterogeneous networks with energy harvesting personal cells-network throughput and energy efficiency,” *IEEE Transactions on Wireless Communications*, vol. 15, no. 2, pp. 1146–1161, Feb 2016.
- [28] Z.-Q. Luo and W. Yu, “An introduction to convex optimization for communications and signal processing,” *IEEE Journal on Selected Areas in Communications*, vol. 24, no. 8, pp. 1426–1438, Aug 2006.
- [29] M. Grant and S. Boyd, “CVX: Matlab software for disciplined convex programming, version 2.1,” <http://cvxr.com/cvx>, Mar. 2014.
- [30] M. Grant, S. Boyd, and Y. Ye, *Disciplined Convex Programming*. Boston, MA: Springer US, 2006, pp. 155–210. [Online]. Available: http://dx.doi.org/10.1007/0-387-30528-9_7
- [31] L. Zhang, Y. C. Liang, and Y. Xin, “Joint beamforming and power allocation for multiple access channels in cognitive radio networks,” *IEEE Journal on Selected Areas in Communications*, vol. 26, no. 1, pp. 38–51, Jan 2008.
- [32] M. Schubert and H. Boche, “Solution of the multiuser downlink beamforming problem with individual sinr constraints,” *IEEE Transactions on Vehicular Technology*, vol. 53, no. 1, pp. 18–28, Jan 2004.
- [33] W. Yang and G. Xu, “Optimal downlink power assignment for smart antenna systems,” in *Acoustics, Speech and Signal Processing, 1998. Proceedings of the 1998 IEEE International Conference on*, vol. 6, May 1998, pp. 3337–3340 vol.6.